

The topology of Gelfand–Zeitlin fibers

Jeffrey D. Carlson and Jeremy Lane

September 27, 2022

Abstract

We prove several new results about the topology of fibers of Gelfand–Zeitlin systems on unitary and orthogonal coadjoint orbits, at the same time finding a unifying framework recovering and shedding light on essentially all known results. We find completely explicit descriptions of the diffeomorphism type of the fiber in many instances a direct factor decomposition of the fiber, and a torus factor corresponding to the action given by the Thimm trick. The new description also gives us a weak local normal form for a coadjoint orbit, which we use to define a topological toric degeneration, new in the orthogonal case,

We also compute the first three homotopy groups (new in the orthogonal case) and cohomology rings of a fiber (new in both cases). All these descriptions can be read in a straightforward manner from the combinatorics of the associated Gelfand–Zeitlin pattern.

1. Introduction

Gelfand–Zeitlin systems are a family of completely integrable systems named for their connection to Gelfand–Zeitlin canonical bases [GS83a],¹ orthogonal Lie groups. The fibers of their moment maps, or *Gelfand–Zeitlin fibers*, are interesting from several perspectives, such as geometric quantization [GS83a, HK14], Floer theory [NNU10, NU16, CKO20], and the topology of integrable systems on symplectic manifolds [BMMT18, Problem 2.9]. The moment map images of Gelfand–Zeitlin systems on unitary and orthogonal coadjoint orbits are polytopes known as *Gelfand–Zeitlin polytopes* whose faces are enumerated by combinatorial diagrams called *Gelfand–Zeitlin patterns*² (see Figure 1.0.4). The Gelfand–Zeitlin (henceforth GZ) fiber over a given point is naturally associated with the GZ pattern of the face of the GZ polytope containing the point in its interior.

In recent work, Cho, Kim and Oh observed that both unitary and orthogonal GZ fibers are total spaces of certain towers of fiber bundles [CKO20, CK20]. They used this description to show that every unitary GZ fiber decomposes as a direct product of a torus and a space whose first and second homotopy groups are trivial. They were also able to explicitly describe the fibers in each stage of their towers as certain products of spheres determined by the combinatorics of the associated pattern. In particular, their results give a combinatorial formula for the dimension of a fiber in terms of the associated pattern. Unitary GZ fibers were also studied by Bouloc, Miranda, and Zung from a very different perspective [BouMZ18]. In addition to recovering an equivalent dimension counting formula, they show that every unitary GZ fiber admits a product decomposition, finer than Cho–Kim–Oh’s, in which direct factors are enumerated by connected components of the associated GZ pattern. In the case where a connected component is a diamond, they are

¹ The name “Zeitlin” is variously romanized in the literature, also appearing as “Cetlin” and “Tsetlin.”

² Some authors prefer to use ladder diagrams, which are equivalent.

able to simplify their description of the corresponding factor to show that it is diffeomorphic to a unitary group.

Although these recent results have greatly improved our understanding of GZ fibers, they do not provide a clear description of the topology of GZ fibers in all cases. For example, it is not clear how to extract from these results a simple, useful description of the diffeomorphism type of the GZ fiber corresponding to more complicated patterns such as that of Figure 1.0.4. This brings us to our first result. We modify Cho–Kim–Oh’s tower construction to show that every unitary and orthogonal GZ fiber can also be expressed as a balanced product, that is, a quotient of the form

$$\begin{aligned} H_\alpha \times H_{\alpha+1} \times \cdots \times H_n / L_\alpha \times L_{\alpha+1} \times \cdots \times L_n, \\ (h_\alpha, h_{\alpha+1}, \dots, h_n) \sim (h_\alpha \ell_\alpha^{-1}, \psi_\alpha(\ell_\alpha) h_{\alpha+1} \ell_{\alpha+1}^{-1}, \dots, \psi_{n-1}(\ell_{n-1}) h_n \ell_n^{-1}), \end{aligned} \quad (1.0.1)$$

where the groups H_k and L_k are certain products of unitary and orthogonal groups determined by the GZ pattern and $\psi_k: L_k \rightarrow H_{k+1}$ are certain injective homomorphisms (see Theorem 3.4.3). It follows immediately from this description that every GZ fiber is a direct product whose factors correspond to connected components of the GZ pattern, a result which is new in the orthogonal case (see Corollary 3.5.1). More importantly, we are able to systematically simplify the expressions (1.0.1) in terms of the combinatorics of the associated GZ pattern. As a result of this simplification, we are able to provide relatively succinct descriptions of the diffeomorphism types of all GZ fibers, even those with relatively complex GZ patterns such as in Figure 1.0.4 (see Example 1.0.3 below). We illustrate these results with a number of examples (Examples 3.5.14–3.5.22). In particular, our results recover the descriptions of elliptic non-degenerate singular fibers and multi-diamond singular fibers given by Bouloc *et al.* as special cases.

Our decomposition also allows us to extract torus factors from a GZ fiber with almost no effort, not only in the unitary case, but also now in the orthogonal case (Section 3.6). These torus factors are associated with a free torus action on each torus, which we are able to identify with the action induced by the Thimm trick (Theorem 3.6.9). Moreover, our decomposition leads to weak local expressions for a coadjoint orbit (Sections 4.2 and 4.3) which allow us to parlay the extraction of our tori into a topological model for a toric degeneration (Theorem 4.1.3). That such degenerations exist was known for unitary GZ systems [NNU10], but an analogue for orthogonal GZ systems seems to remain open.

The decomposition allows us to extract the first three homotopy groups of a unitary or orthogonal Gelfand–Zeitlin fiber from the GZ pattern with little effort (Section 5.1). We find that orthogonal fibers split as a product of a torus and a space whose first and second homotopy groups have the forms $(\mathbb{Z}/2)^s$ and \mathbb{Z}^f respectively. We also show that the third homotopy groups of unitary and orthogonal GZ fibers are free abelian (Propositions 5.1.2 and 5.1.3). With a more substantial effort, we can also compute the cohomology rings of arbitrary fibers of unitary and orthogonal GZ systems (Sections 5.2 and 5.3). We may briefly summarize these results as follows.

Theorem 1.0.2. *The integral cohomology of a unitary Gelfand–Zeitlin fiber is an exterior algebra on odd-degree generators. The cohomology of an orthogonal Gelfand–Zeitlin fiber over $\mathbb{Z}[1/2]$ is also an exterior algebra; the integral and mod-2 cohomology groups are isomorphic to those of a product of real Stiefel manifolds.*

The degrees of the relevant generators and the precise relevant Stiefel manifolds are again determined in a straightforward manner from the associated GZ pattern; see Theorems 5.2.1 and 5.3.12

for more detail. The cohomology rings of these Stiefel manifolds is also known [ČaMV03], so our description gives much but not all of the integral cohomology ring structure for the GZ fiber. These cohomology computations follow inductively from an analysis of the Serre spectral sequences associated to Cho–Kim–Oh’s towers. Surprisingly, the spectral sequence associated to each bundle collapses in the unitary case, and moreover, as the cohomology of base and fiber for each bundle are exterior algebras, there is no extension problem, additively or multiplicatively. In the orthogonal case, the spectral sequences associated to the sphere bundles do not typically collapse, but those associated to allied Stiefel manifold bundles do.

Example 1.0.3. Consider the GZ pattern in Figure 1.0.4. Using our results, one can immediately read from this pattern that an associated GZ fiber is diffeomorphic to

$$(S^1)^7 \times (S^3)^3 \times \mathrm{U}(2) \backslash (\mathrm{U}(4) \times \mathrm{U}(3)) / \mathrm{U}(2),$$

has integral cohomology ring isomorphic to

$$\Lambda[z_{1,1}, z_{1,2}, z_{1,3}, z_{1,4}, z_{1,5}, z_{1,6}, z_{1,7}, z_{3,1}, z_{3,2}, z_{3,3}, z_{5,1}, z_{5,2}, z_{7,1}], \quad |z_{m,j}| = m,$$

and has $\pi_3 \cong \mathbb{Z}^3$. See Examples 3.5.22 and 5.2.2 for more details.

We end this introduction with a discussion of the broader context and motivation for our work. Gelfand–Zeitlin systems are useful and interesting because they share many features with toric integrable systems (convexity and global action-angle coordinates) but have non-toric singularities. They form part of a larger family of examples with similar behaviour that also includes bending flow systems on polygon space [KapM96], Goldman systems on moduli space [Gold86], and integrable systems constructed by toric degeneration [HK15] (of which GZ systems are an example [NNU10]). This family of examples continues to grow. For instance, the construction of integrable systems by toric degeneration was recently extended [HL20], and as a consequence, it was shown that every coadjoint orbit of every compact, connected Lie group admits integrable systems that share the features of GZ systems mentioned above.

There are many questions regarding the non-toric singularities of these systems which are currently unanswered. For example, it is known in the cases of bending flow systems [Bou18] and GZ systems [BouMZ18, CKO20] that the non-toric fibers are isotropic (this result is expected to have applications in Lagrangian Floer theory [CKO20]), but it is not known whether non-toric fibers of integrable systems constructed by toric degeneration are isotropic in general (this is conjectured to be true by Bouloc *et al.* [BouMZ18]). Similarly, very little is known in general about the topology of non-toric fibers of integrable systems constructed by toric degeneration. There is also the problem of finding local normal forms for the non-toric singularities of these systems, as motivated by Bolsinov *et al.* for the case of GZ systems [BMMT18, Problem 2.9]. At the moment, very little is known about this problem, even in the case of the more concrete GZ systems, with the exception of several examples in low dimension studied by Alamiddine [Ala09]. Progress on any of these questions would have further applications in symplectic topology, geometric quantization, and the topology of integrable systems.

To give a particularly concrete example of one such application, we end by describing one of the original motivations for studying GZ systems (and a potential future application of this work). Guillemin and Sternberg observed that if integral points in the boundary of an integral GZ polytope are formally included in the Bohr–Sommerfeld set, then the dimension of the resulting Bohr–Sommerfeld quantization equals the dimension of the Kähler quantization of the coadjoint

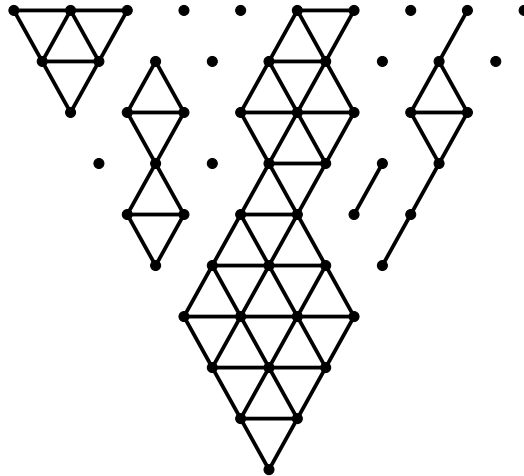


Figure 1.0.4: Example of a GZ pattern associated to a fiber of a GZ system on a non-regular coadjoint orbit of $U(10)$.

orbit [GS83a]. In ongoing work, we plan to use our description of the topology of the singular GZ fibers, and a description of a local model for the GZ systems in neighbourhoods of said fibers, to give a more principled justification of Guillemin and Sternberg’s observation, i.e., to prove that a singular fiber is Bohr–Sommerfeld if and only if it is integral. Moreover, we hope to extend the results of Hamilton–Kono [HK14] by showing that holomorphic sections in the Kähler quantization that correspond to boundary points of the GZ polytope converge under a deformation of complex structure to distributional sections supported on the singular fibers over the same boundary points.

Organization of the paper. In Section 2, we recall the description of GZ fibers as towers. In particular, we recall results of Cho–Kim–Oh which describe the bundles of homogeneous spaces that occur at each stage in terms of the associated GZ pattern [CKO20, CK20]. We note a minor correction to Cho and Kim’s description [CK20] of the bundles in the orthogonal case (although this correction does not impact their final results, it does play an important role in our account). Section 3 contains our description of the GZ fibers as biquotients (Theorem 3.4.13). This presentation shows that GZ fibers decompose as direct products of factors indexed by components of the associated GZ pattern. We provide examples demonstrating how easily our biquotient description can be read from the associated GZ pattern. We also demonstrate how this description enables us to recover a direct torus factor, and relatedly a torus action and a (topological) toric degeneration; this last depends on the weak local normal forms over the interior of a face and the interiors of two adjoining faces developed in Section 4. In Section 5.1, we use this description to determine the first three homotopy groups of a GZ fiber. In Section 5.2, we state and prove the main theorem (Theorem 5.2.1) regarding cohomology of GZ fibers in the unitary case. Finally, Section 5.3 contains our cohomological results in the orthogonal case.

Acknowledgements. Both authors were supported by a Fields Postdoctoral Fellowship associated with the 2020 Thematic Program in Toric Topology during the original collaborative work that lead to this manuscript.

2. Gelfand–Zeitlin systems and Gelfand–Zeitlin fibers

This section recalls the Gelfand–Zeitlin systems on unitary and orthogonal coadjoint orbits as well as the description of their fibers as towers. In order to avoid repeating ourselves, we begin in Section 2.1 by giving a general description of GZ systems and fibers that applies equally in both cases. We recall the details that are specific to the unitary and orthogonal cases in Sections 2.2 and 2.3 respectively.

For further details regarding GZ systems, we direct the reader to the original papers of Guillemin and Sternberg [GS83a, GS83b] and the recent papers of Cho–Kim–Oh describing the GZ fibers as towers of bundles of homogeneous spaces [CK20, CKO20]. As mentioned in the introduction, an alternative description of the GZ fibers is given by Bouloc *et al.* [BouMZ18]. We also remark that the Ph.D. thesis of Milena Pabiniak [Pab12] contains many useful details.

2.1. Some known facts and set-up in the general case

This section recalls why fibers of both unitary and orthogonal Gelfand–Zeitlin systems are towers of bundles of homogeneous spaces, in terms of a much more general set-up.

Definition 2.1.1. Let positive integers $\alpha < n$ be given along with G_k ($\alpha \leq k \leq n+1$) topological groups connected by injective homomorphisms $\varphi = \varphi_k: G_k \rightarrow G_{k+1}$ ($\alpha \leq k \leq n$) and G_k -spaces V_k ($\alpha \leq k \leq n+1$) connected by maps $\Phi = \Phi_{k+1}: V_{k+1} \rightarrow V_k$ ($\alpha \leq k \leq n$). We write $\mathcal{O}_{\vartheta^{(k)}} := G_k \cdot \vartheta^{(k)}$ for the orbit of $\vartheta^{(k)} \in V_k$ and suppose that

- Each Φ_{k+1} is φ_k -equivariant in the sense that for all $g_k \in G_k$ and $\vartheta^{(k+1)} \in V_{k+1}$,

$$\Phi_{k+1}(\varphi_k(g_k)\vartheta^{(k+1)}) = g_k\Phi_{k+1}(\vartheta^{(k+1)});$$

- The group $\varphi_k(G_k) \leq G_{k+1}$ acts transitively on any nonempty intersection $\mathcal{O}_{\vartheta^{(k+1)}, \vartheta^{(k)}} := \mathcal{O}_{\vartheta^{(k+1)}} \cap \Phi^{-1}(\mathcal{O}_{\vartheta^{(k)}})$.

Fix $\vartheta^{(n+1)} \in V_{n+1}$ and write $\mathcal{O} = \mathcal{O}_{\vartheta^{(n+1)}}$. Taking orbits of iterated Φ -images yields a natural map

$$\begin{aligned} \Psi: \mathcal{O} &\longrightarrow \prod_{k=\alpha}^n V_k/G_k =: \Delta, \\ \vartheta^{(n+1)} &\longmapsto (\mathcal{O}_{\Phi^{n+1-k}(\vartheta^{(n+1)})})_{k=\alpha}^n. \end{aligned}$$

We call the map Ψ a *topological Gelfand–Zeitlin system* and will attempt to characterize the *Gelfand–Zeitlin fiber* $\Psi^{-1}(p)$ over a point $p = (\bar{\lambda}^{(k)})_{k=\alpha}^n \in \Delta \cap \text{im } \Psi$.

Definition 2.1.2. If $\varphi_k: G_k \rightarrow G_{k+1}$ are injective Lie group homomorphisms, $V_k = \mathfrak{g}_k^*$ the coadjoint representations, and $\Phi_{k+1} = \varphi_k^*: \mathfrak{g}_{k+1}^* \rightarrow \mathfrak{g}_k^*$ the cotangent maps, Ψ from Definition 2.1.1 is called a *Gelfand–Zeitlin system*. We will call a map defined in the general context *smooth* if it becomes smooth in the case of a GZ system. The main cases are the *unitary* and *orthogonal GZ systems* with $G_k = \text{U}(k)$ or $\text{SO}(k)$ and $\alpha = 1$ or 2 (respectively) and each φ_k a block inclusion $g \mapsto \begin{bmatrix} g & \\ & 1 \end{bmatrix}$.

Fix a maximal torus T_k in each G_k , and fix positive Weyl chambers $\mathfrak{t}_{k,+}^*$ in the linear duals \mathfrak{t}_k^* of their Lie algebras. Since each $\text{Ad}_{G_k}^*$ -orbit on $V_k = \mathfrak{g}_k^*$ meets $\mathfrak{t}_{k,+}^*$ in precisely one point, we identify $\mathfrak{t}_{k,+}^*$ with the orbit space $V_k/G_k = \mathfrak{g}_k^*/G_k$, making Ψ a map $\mathcal{O} \rightarrow \prod_{k=\alpha}^n \mathfrak{t}_{k,+}^*$. We will write $\lambda^{(k)}$ for points of $\mathfrak{t}_{k,+}^*$, so that we are interested in the spaces $\Psi^{-1}(\lambda^{(n)}, \dots, \lambda^{(1)})$.

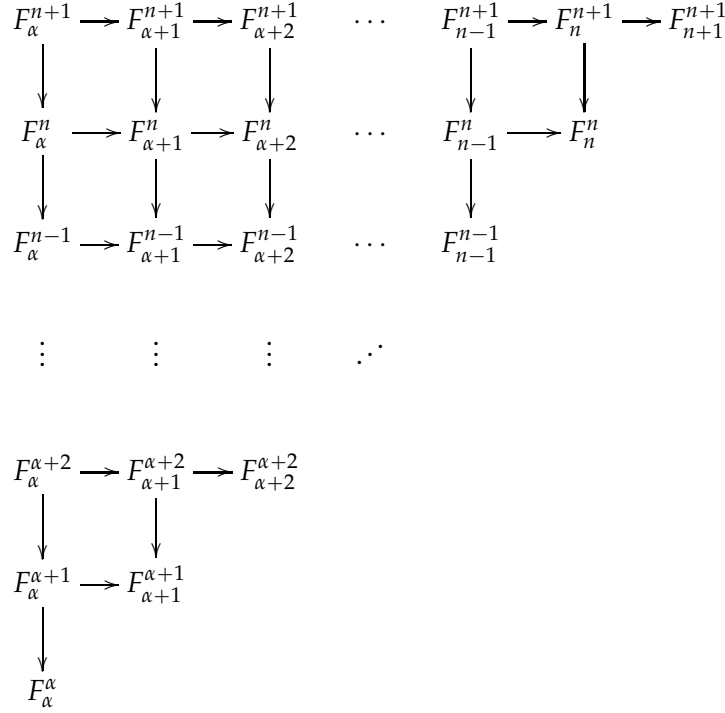


Figure 2.1.3: Gelfand–Zeitlin fibers can be viewed as the total space F_α^{n+1} of a tower of fiber bundles (on the left side of the diagram) which is constructed through a sequence of pullbacks.

Remark 2.1.4. Guillemin and Sternberg showed that a unitary or orthogonal Gelfand–Zeitlin system Ψ generates a Hamiltonian action of $T_n \times \cdots \times T_\alpha$ on an open, dense subset of $\mathcal{O}_{\lambda^{(n+1)}}$, with respect to the canonical Kostant–Kirillov–Souriau symplectic structure on $\mathcal{O}_{\lambda^{(n+1)}}$ [GS83a]. They also showed in these cases that the map Ψ defined in (2.1.1) is a GZ system on any coadjoint orbit $\mathcal{O}_{\lambda^{(n+1)}}$ [GS83b]. In both cases, the resulting densely defined torus action is completely integrable, or toric, for every $\lambda^{(n+1)}$ in $\mathfrak{t}_{n+1,+}^*$. It was shown in a more general setting by the second author that the dense subset where Ψ generates a torus action is connected and the fibers of Ψ are all connected [Lane18].

2.1.5 (The staircase and pullbacks). Following Definition 2.1.2, for each $p = (\bar{\lambda}^{(k)}) \in \Delta$ we fix orbit representatives $\lambda^{(k)} \in V_k$ of $\bar{\lambda}^{(k)}$ for all k . (In the cases of unitary and orthogonal systems, there will be very natural such choices, amounting to a continuous section.) To say a point $\vartheta^{(n+1)} \in V_{n+1}$ lies in $\Psi^{-1}(p)$ means that each $\vartheta^{(k)} := \Phi^{n+1-k}(\vartheta^{(n+1)})$ lies in $\mathcal{O}_{\lambda^{(k)}}$, and that each $\vartheta^{(k+1)}$ lies in $\mathcal{O}_{\lambda^{(k+1)}, \lambda^{(k)}}$. Conversely, we can ask when a system $(\zeta^{(k)}) \in \prod \mathcal{O}_{\lambda^{(k+1)}, \lambda^{(k)}}$ comes from some $\vartheta^{(n+1)}$. Let $\Psi_i: V_k \rightarrow V_i/G_i$ be the composite of $\Phi^{k-i}: V_k \rightarrow V_i$ and the projection, for any $i \leq k$. For $\alpha \leq j \leq k \leq n+1$, we denote by $F_j^k \subseteq V_k$ the space of points $\zeta^{(k)}$ with $\Psi_i(\zeta^{(k)}) = \lambda^{(i)}$ for $j \leq i \leq k$. Then $\Psi^{-1}(p) = F_\alpha^{n+1}$. Following Cho–Kim–Oh [CKO20], these all fit together into the system shown in Figure 2.1.3, in which all horizontal maps are inclusion and all vertical maps are Φ . Each rectangle in Figure 2.1.3 in fact represents a fiber product in a natural way.³ Since each rectangle is a fiber product, this means $\Psi^{-1}(p)$ can be calculated inductively as the an iterated fiber product if we can just understand the maps in Figure 2.1.3.

³ Indeed, for $i < j < k < m$, if $\zeta^{(k)} \in F_i^k \subseteq F_j^k$ is the image under Φ^{m-k} of $\zeta^{(m)} \in F_j^m$, then it means $\Psi_s(\zeta^{(m)}) = \lambda^{(s)}$ for $i \leq s \leq k$ as well as for $j \leq s \leq m$.

2.1.6 (Stabilizers and the vertical maps). We work in the context of a topological Gelfand–Zeitlin system with orbit representatives $\lambda^{(k)}$ chosen as in 2.1.5, summarizing the work of Cho–Kim–Oh.⁴ For each $k \leq n$, fix $\zeta^{(k+1)} \in \mathcal{O}_{\lambda^{(k+1)}} \cap \Phi^{-1}(\lambda^{(k)})$.⁵ We write

$$L_k := \varphi^{-1}(\text{Stab}_{G_{k+1}} \zeta^{(k+1)}) \leq \text{Stab}_{G_k} \lambda^{(k)} =: H_k.$$

Then $\mathcal{O}_{\lambda^{(k)}} = G_k \cdot \lambda^{(k)}$ is diffeomorphic to G_k/H_k by the orbit–stabilizer theorem. Since we have assumed the action of $\varphi(G_k)$ on $\mathcal{O}_{\lambda^{(k+1)}, \lambda^{(k)}}$ is transitive, we see $\mathcal{O}_{\lambda^{(k+1)}, \lambda^{(k)}}$ is diffeomorphic to G_k/L_k , and the fiber of the restriction $\Phi: \mathcal{O}_{\lambda^{(k+1)}, \lambda^{(k)}} \rightarrow \mathcal{O}_{\lambda^{(k)}}$ over $\lambda^{(k)}$ itself can be identified with H_k/L_k . In the case of a GZ system, since all groups are Lie groups, it is well known that

$$H_k/L_k \rightarrow G_k/L_k \rightarrow G_k/H_k \tag{2.1.7}$$

is a fiber bundle. Thus from Figure 2.1.3, in which every rectangle now represents a pullback of fiber bundles, we see that $\Psi^{-1}(p)$ is an iterated fiber bundle with fibers $H_\alpha/L_\alpha, \dots, H_n/L_n$.

2.2. The unitary case

This section establishes notation and describes the groups $L_k \leq H_k \leq G_k$ of 2.1.6 for unitary Gelfand–Zeitlin systems following Cho–Kim–Oh [CKO20].

2.2.1. Recall from Definition 2.1.2 that in this case $G_k = \text{U}(k)$ for $1 \leq k \leq n+1$. The coadjoint representation $\mathfrak{u}(k)^*$ can be identified with the conjugation action of $\text{U}(k)$ on the space of $k \times k$ Hermitian matrices.⁶ Then $\Phi_{k+1} = \varphi_k^*$ becomes the truncation map extracting from a $(k+1) \times (k+1)$ matrix its upper-left $k \times k$ submatrix. We select the diagonal matrices of $\text{U}(k)$ as the maximal torus T_k ; then the positive Weyl chamber $\mathfrak{t}_{k,+}^*$ can be identified with the set of points $\lambda^{(k)} = (\lambda_1^{(k)}, \dots, \lambda_k^{(k)}) \in \mathbb{R}^k$ with $\lambda_1^{(k)} \geq \dots \geq \lambda_k^{(k)}$, so that the coadjoint orbit $\mathcal{O}_{\lambda^{(k)}}$ is the set of $k \times k$ Hermitian matrices with eigenvalues, listed in weakly decreasing order, $\lambda_1^{(k)}, \dots, \lambda_k^{(k)}$.

2.2.2 (The GZ polytope and GZ patterns). It is a result of linear algebra that $\mathcal{O}_{\lambda^{(k+1)}, \lambda^{(k)}}$ is non-empty if and only if $\lambda^{(k)}$ and $\lambda^{(k+1)}$ satisfy *interlacing inequalities*

$$\begin{array}{ccccccccc} \lambda_1^{(k+1)} & & \lambda_2^{(k+1)} & & \lambda_3^{(k+1)} & & \lambda_k^{(k+1)} & & \lambda_{k+1}^{(k+1)} \\ & \searrow & & \searrow & & \searrow & & \searrow & \\ & \lambda_1^{(k)} & & \lambda_2^{(k)} & & \dots & & \lambda_k^{(k)} & \end{array} \tag{2.2.3}$$

The image of the GZ system on $\mathcal{O}_{\lambda^{(n+1)}}$ is the set $\Delta = \Delta_{\lambda^{(n+1)}}$ of those points in $\prod_{k=1}^n \mathbb{R}^k \cong \mathbb{R}^{n(n+1)/2}$ whose coordinates $\lambda_j^{(k)}$ ($1 \leq j \leq k \leq n$) satisfy the interlacing inequalities (2.2.3) for all k [GS83a]. Since each inequality cuts out a half-space, it follows $\Delta \subsetneq \mathbb{R}^{n(n+1)/2}$ is a polytope, called the *unitary Gelfand–Zeitlin polytope* associated to $\lambda^{(n+1)}$. We represent these inequalities

⁴ With (N.B.) somewhat different notation and emphases. For example, they do not seem to explicitly state (2.1.7) is a bundle of homogeneous spaces, though it follows from their analysis, but this will be crucial for us.

⁵ This is possible as, since we assume p lies in $\text{im } \Psi$, we have $\lambda^{(k)} \in G_k \cdot \Phi(\zeta^{(k+1)})$ for some $\zeta^{(k+1)} \in G_{k+1} \cdot \lambda^{(k+1)}$, and hence there is some g_k with $\lambda^{(k)} = g_k \cdot \Phi(\zeta^{(k+1)}) = \Phi(\varphi(g_k)\zeta^{(k+1)})$.

⁶ It would be more natural, but less convenient, to consider the space skew-Hermitian matrices, which is equivariantly isomorphic under multiplication by i .

in a triangular array, such as the following pattern for the case $n = 2$.

$$\begin{array}{ccccc}
 \lambda_1^{(3)} & & \lambda_2^{(3)} & & \lambda_3^{(3)} \\
 \Downarrow & \nearrow & \Downarrow & \nearrow & \\
 & \lambda_1^{(2)} & & \lambda_2^{(2)} & \\
 & \Downarrow & & \nearrow & \\
 & & \lambda_1^{(1)} & &
 \end{array} \tag{2.2.4}$$

To each point in $p = (\lambda^{(k)}) \in \Delta_{\lambda^{(n+1)}}$, we associate its *unitary Gelfand–Zeitlin pattern*, a graded planar graph constructed from the triangular array of inequalities, by replacing each number $\lambda_j^{(k)}$ with a vertex and drawing an edge between two nearest-neighbour vertices (in the same row or adjacent rows) if and only if the associated $\lambda_j^{(k)}$ are equal.⁷ Such a graph will look something like Figure 1.0.4. Note that the pattern of p depends only on the face of Δ containing p in its interior and not on the particular values $\lambda_j^{(k)}$.

2.2.5 (Rows and the groups H_k). *Row k* of a unitary GZ pattern is the full subgraph on the row of vertices corresponding to the numbers $\lambda_1^{(k)}, \dots, \lambda_k^{(k)}$; this linear graph will comprise a number (call it $\ell = \ell_k$) of component segments each corresponding to a distinct entry of $\lambda^{(k)}$. If d_i ($1 \leq i \leq \ell$) is the number of vertices in the i^{th} component from the left, the centralizer of the canonical diagonal orbit representative $\lambda^{(k)}$ from 2.2.1 is the block-diagonal subgroup

$$H_k = \mathrm{U}(d_1) \oplus \cdots \oplus \mathrm{U}(d_\ell) \leq \mathrm{U}(k). \tag{2.2.6}$$

2.2.7 (Representatives $\zeta^{(k+1)}$ and groups L_k ; trapezoids and parallelograms). Continuing with the notation of 2.2.5, let μ_i be the distinct entries of $\lambda^{(k)}$, in decreasing order. An element of $\Phi^{-1}(\lambda^{(k)}) \cap \mathcal{O}_{\lambda^{(k+1)}}$, as in 2.1.6, is then constrained to be of the block form

$$\zeta^{(k+1)} = \left[\begin{array}{c|c|c|c}
 \text{diag}(\mu_1, \dots, \mu_1) & & & z_1 \\
 & \ddots & & \vdots \\
 & & \text{diag}(\mu_\ell, \dots, \mu_\ell) & z_\ell \\
 \hline
 \bar{z}_1^\top & \cdots & \bar{z}_\ell^\top & c
 \end{array} \right]. \tag{2.2.8}$$

Here, because trace is a conjugacy invariant, we must have $c = \text{tr } \lambda^{(k+1)} - \text{tr } \lambda^{(k)} \in \mathbb{R}$, and we will show momentarily that the squares of the Euclidean norms $r_i = \|z_i\|^2$ of $z_i \in \mathbb{C}^{d_i}$ are also rational functions of (and hence continuous in) the entries $\lambda^{(k)}$ and $\lambda^{(k+1)}$.

For an element $h_k = u_1 \oplus \cdots \oplus u_\ell \in H_k$, one checks the conjugation action of $\varphi(h_k)$ on $\zeta^{(k+1)}$ fixes the diagonal entries and replaces each column vector z_i with $u_i \cdot z_i$. Since $\mathrm{U}(d_i)$ acts transitively on the sphere of radius r_i in \mathbb{C}^{d_i} , we see H_k/L_k is diffeomorphic to the product of spheres $\prod_{r_i \neq 0} S^{2d_i-1}$. We usually choose $\zeta^{(k+1)}$ so that $z_i = [r_i \ 0 \ \cdots \ 0]^\top$ (whether or not $r_i = 0$). For this choice, the group $L_k \leq H_k$ such that $L_k \oplus [1]$ centralizes $\zeta^{(k+1)}$ is the block sum

$$L_k = K_1 \oplus \cdots \oplus K_\ell \leq \mathrm{U}(d_1) \oplus \cdots \oplus \mathrm{U}(d_\ell) = H_k, \tag{2.2.9}$$

where $K_i \leq \mathrm{U}(d_i)$ is $\mathrm{U}(d_i)$ itself when $r_i = 0$ and $[1] \oplus \mathrm{U}(d_i - 1)$ when $r_i > 0$.

⁷ These are equivalent to the *ladder diagrams* of Cho–Kim–Oh. To convert from one of our GZ patterns to a ladder diagram, draw a grid in gray such that each $\lambda_j^{(k)}$ lies in a (diamond) box, and for each strict inequality, which will cross one grey box edge, color that edge black. Then remove the top row of entries $\lambda_j^{(n+1)}$ and rotate the diagram by $-\pi/4$ so that $\lambda_1^{(1)}$ is at the lower-left.

This dichotomy can be interpreted usefully in terms of the GZ pattern. Consider the full subgraph of the GZ pattern on the vertices of rows k and $k + 1$. A connected component of this subgraph will be called a \triangle -shape if it has more vertices in row k , a ∇ -shape if it has more in row $k + 1$, and a \square -shape if it contains the same number in each row.⁸ Since a nonzero r_i forces down the multiplicity of μ_i as an eigenvalue of $\zeta^{(k+1)}$, while $r_i = 0$ guarantees an multiplicity of at least d_i , it follows that a \triangle -shape corresponds to $K_i = [1] \oplus U(d_i)$ while a \square - or ∇ -shape corresponds to $K_i = U(d_i)$. Hence sphere factors of H_k/L_k arise from \triangle -shapes in the pattern.

We will need the formula for r_i^2 . Write λ_s for the distinct entries of $\lambda^{(k+1)}$ and equate the characteristic polynomials of $\lambda^{(k+1)}$ and $\zeta^{(k+1)}$ (expanding by minors along the last column for ζ). Dividing out common factors $x - \lambda_j^{(k+1)}$ and evaluating at $x = \mu_i$ shows that if μ_i belongs to a ∇ - or \square -shape in the k^{th} and $(k + 1)^{\text{st}}$ rows of the GZ pattern, then $r_i = 0$, and otherwise

$$r_i^2 = -\frac{\prod_w (\mu_i - \lambda_w)}{\prod_{m \neq i} (\mu_i - \mu_m)}, \quad (2.2.10)$$

where the indices w run over ∇ -shapes and the m run over \triangle -shapes.

Remark 2.2.11. In exceptional situations later, we will use a representative $'\zeta^{(k+1)}$ as in 2.2.7 which is like our usual choice of $\zeta^{(k+1)}$ except that $z'_i = [0 \cdots 0 r_i]^\top$ and the corresponding block factor of its stabilizer L'_k is $U(d_i - 1) \oplus [1]$. Note that $'\zeta^{(k+1)} = \varphi_k(h)\zeta^{(k+1)}$ for a block-unitary matrix $h = u_1 \oplus \cdots \oplus u_\ell \in H_k \in \prod_{i=1}^\ell \text{SU}(d_i)$.⁹

Example 2.2.12. Consider the unitary GZ pattern in Figure 1.0.4. Looking at rows 4 and 5, we see that $H_4 = U(4)$ and $L_4 = [1] \oplus U(3)$. Looking at rows 6 and 7, we see that

$$H_6 = U(2) \oplus U(2) \oplus U(1) \oplus U(1), \quad L_6 = ([1] \oplus U(1)) \oplus U(2) \oplus U(1) \oplus U(1).$$

Looking at the penultimate row 9, we see $H_9 \cong U(2) \oplus U(1)^{\oplus 2} \oplus U(2) \oplus U(1)^3$ whereas $L_9 \cong U(2) \oplus U(0)^2 \oplus U(2) \oplus U(0) \oplus U(1) \oplus U(0)$. We only look at row 10 in conjunction with row 9 to determine what the \triangle -, ∇ -, and \square -shapes are; while H_{10} is defined, L_{10} is not. Correspondingly, it does not make sense to refer to \triangle -shapes in row 10, since there is no row 11.

2.3. The orthogonal case

This section establishes notation and describes the groups $L_k \leq H_k \leq G_k$ of 2.1.6 for orthogonal Gelfand–Zeitlin systems, mostly following Cho–Kim [CK20].¹⁰ Throughout this section, we write $[k]$ for $\lfloor k/2 \rfloor$, where $\lfloor \cdot \rfloor$ is the floor function.

2.3.1. Recall from Definition 2.1.2 that in this case $G_k = \text{SO}(k)$ for $2 \leq k \leq n + 1$. The coadjoint representations $\mathfrak{so}(k)^*$ can be identified with the conjugation action of $\text{SO}(k)$ on the space of $k \times k$ skew-symmetric matrices. Again $\Phi_{k+1} = \varphi_k^*$ becomes the truncation map extracting from

⁸ The terminology of \square -shape/ ∇ -shape/ \triangle -shape is equivalent to the N-block/W-block/M-block trichotomy used for the ladder diagrams of Cho–Kim–Oh [CKO20].

⁹ For example, this can be taken such that u_s is the identity matrix for $s \neq i$ and $u_i \in U(d_i)$ is \pm -signed permutation matrix with a 1 in the first column.

¹⁰ The description of the subgroups H_k and L_k given here diverges slightly from theirs [CK20, Lem. 6.5], which gives blocks $\text{SO}(2d_i)$ where we find $U(d_i)$. As $\text{SO}(2d_i)/\text{SO}(2d_i - 1)$ and $U(d_i)/U(d_i - 1)$ are both diffeomorphic to $S^{2d_i - 1}$, the quotients H_k/L_k they give are fortunately correct anyway, so this minor error does not affect the rest of their results, but the distinction will be important for us.

a $(k+1) \times (k+1)$ matrix its upper-left $k \times k$ submatrix. We select the block-diagonal matrices $\mathrm{SO}(2)^{\oplus[k]}$ as the maximal torus T_k for k even, and $\mathrm{SO}(2)^{\oplus[k]} \oplus [1]$ for k odd, and write $\beta(\lambda) := \begin{bmatrix} 0 & -\lambda \\ \lambda & 0 \end{bmatrix}$ for $\lambda \in \mathbb{R}$. Under this identification, \mathfrak{t}_k^* is for k even the space of matrices of the block-diagonal form $\bigoplus_{j=1}^{[k]} \beta(\lambda_j)$ for various $\lambda_j \in \mathbb{R}$, and for k odd of matrices $\bigoplus_{j=1}^{[k]} \beta(\lambda_j) \oplus [1]$. The standard positive Weyl chamber $\mathfrak{t}_{k,+}^*$ is the set of such matrices with

$$\begin{aligned} \lambda_1^{(k)} &\geq \lambda_2^{(k)} \geq \dots \geq \lambda_{[k]-1}^{(k)} \geq |\lambda_{[k]}^{(k)}|, & k \text{ even,} \\ \lambda_1^{(k)} &\geq \lambda_2^{(k)} \geq \dots \geq \lambda_{[k]-1}^{(k)} \geq \lambda_{[k]}^{(k)} \geq 0, & k \text{ odd.} \end{aligned} \quad (2.3.2)$$

For brevity, we abusively write the standard conjugacy class representatives in $\mathfrak{t}_{k,+}^*$ again as $\lambda^{(k)}$. Each of these $\lambda_j^{(k)}$ corresponds to the pair of complex conjugate eigenvalues $\pm i\lambda_j^{(k)}$; for k odd there is also one additional instance of 0 in the list of eigenvalues.

2.3.3 (The GZ polytope and GZ patterns). The interlacing inequalities characterizing for which $\lambda^{(k)}$ and $\lambda^{(k+1)}$ the intersection $\mathcal{O}_{\lambda^{(k+1)}, \lambda^{(k)}}$ is non-empty again¹¹ depend on the parity of k . For k odd, they are

$$\begin{array}{ccccccccc} \lambda_1^{(k+1)} & & \lambda_2^{(k+1)} & & \lambda_3^{(k+1)} & & \lambda_{[k+1]-1}^{(k+1)} & & |\lambda_{[k+1]}^{(k+1)}| \\ \searrow & \nearrow & \searrow & \nearrow & \searrow & \nearrow & \searrow & \nearrow & \searrow \\ & \lambda_1^{(k)} & & \lambda_2^{(k)} & & \dots & & \lambda_{[k]}^{(k)} & & 0 \end{array} \quad (2.3.4)$$

whereas for k even, they are

$$\begin{array}{ccccccccc} \lambda_1^{(k+1)} & & \lambda_2^{(k+1)} & & \lambda_3^{(k+1)} & & \lambda_{[k+1]}^{(k+1)} & & 0 \\ \searrow & \nearrow & \searrow & \nearrow & \searrow & \nearrow & \searrow & \nearrow & \\ & \lambda_1^{(k)} & & \lambda_2^{(k)} & & \dots & & |\lambda_{[k]}^{(k)}| & \end{array} \quad (2.3.5)$$

In both cases, the pattern of inequalities can be extended symmetrically by including 0 and the negatives of the $\lambda_j^{(k)}$, representing $(1/i)$ times all eigenvalues of all truncations.¹² This is thus again represented by a triangular array, such as the following for $n = 4$.

$$\begin{array}{ccccccccc} \lambda_1^{(5)} & & \lambda_2^{(5)} & & 0 & & -\lambda_2^{(5)} & & -\lambda_1^{(5)} \\ \searrow & \nearrow & \searrow & \nearrow & \searrow & \nearrow & \searrow & \nearrow & \\ & \lambda_1^{(4)} & & |\lambda_2^{(4)}| & & -|\lambda_2^{(4)}| & & -\lambda_1^{(4)} & \\ \searrow & \nearrow & \searrow & \nearrow & \searrow & \nearrow & \searrow & \nearrow & \\ & & \lambda_1^{(3)} & & 0 & & -\lambda_1^{(3)} & & \\ \searrow & \nearrow & \searrow & \nearrow & \searrow & \nearrow & & & \\ & & & |\lambda_1^{(2)}| & & -|\lambda_1^{(2)}| & & & \\ \searrow & \nearrow & & \searrow & \nearrow & & & & \\ & & & & 0 & & & & \end{array} \quad (2.3.6)$$

The *orthogonal Gelfand–Zeitlin (GZ) polytope* Δ is the set of points in $\mathbb{R}^{\sum_{k=1}^n [k]}$ for which the coordinates $\lambda_j^{(k)}$ ($1 \leq j \leq [k] < k \leq n$) satisfy all the interlacing inequalities. One passes to a codimension-one face every time a strict inequality becomes an equality.

¹¹ For nonemptiness, see Pabiniak [Pab12, App. B].

¹² One may omit the right side and the zero in the bottom row without loss of information, but we opt to keep these features because they help simplify some descriptions later on.

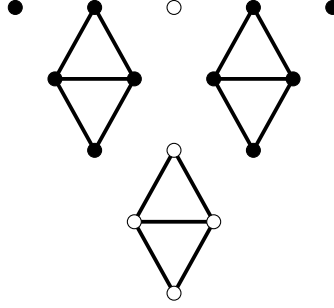


Figure 2.3.8: An orthogonal GZ pattern associated to a fiber of a GZ system on a coadjoint orbit of $\text{SO}(5)$.

Orthogonal Gelfand–Zeitlin (GZ) patterns are obtained from inequality triangles much as in the unitary case. The resulting triangles are symmetric about the vertical midline. For visual salience we colour vertices corresponding to 0 white, although we know vertices along the midline correspond to 0 anyway. The full subgraph on the black vertices to the left of the vertical midline is the **positive part** of the orthogonal GZ pattern and that on the right the **negative part**. The same pattern obtains regardless of whether a given $\lambda_k^{(2k)}$ is positive or negative, so that although the pattern of $p \in \Delta$ depends only on the face of Δ whose interior contains p , the pattern no longer corresponds to just one face.

Example 2.3.7. If in (2.3.6) the values are $\lambda_1^{(5)} = 2$, $\lambda_2^{(5)} = \lambda_1^{(4)} = -\lambda_2^{(4)} = \lambda_1^{(3)} = 1$, and $\lambda_1^{(2)} = 0$, then the GZ pattern is given by Figure 2.3.8.

2.3.9 (Rows and the groups H_k). **Row k** of an orthogonal GZ pattern is again the full subgraph on this row of vertices, comprising some number of component segments. Let ℓ denote the number of connected components of the positive part, each corresponding to a distinct absolute value of an entry of $\lambda^{(k)}$, let d_i ($1 \leq i \leq \ell$) be the number of vertices in the i^{th} component from the left of the positive part, and let d_0 be the number of vertices in the white component.

Then the centralizer H_k of $\lambda^{(k)}$ in $\text{SO}(k)$ is again determined by the GZ pattern and seen to lie in the block sum $\bigoplus_{i=1}^{\ell} \text{SO}(2d_i) \oplus \text{SO}(d_0)$. For $0 < i < \ell$ a block must commute with $\beta(1)^{\oplus d_i}$, forcing it to lie in $\text{Sp}(2d_i, \mathbb{R}) \cap \text{SO}(2d_i)$, which is the image of the embedding $\text{U}(d_i) \rightarrow \text{SO}(2d_i)$ induced by $a + ib \mapsto \begin{bmatrix} a & -b \\ b & a \end{bmatrix}: \mathbb{C} \rightarrow \mathbb{R}^{2 \times 2}$. The same holds for the ℓ^{th} block if k is odd or $k = 2m$ is even with $\lambda_m^{(2m)} \neq -\lambda_{m-1}^{(2m)}$. If however $k = 2m$ with $\lambda_m^{(2m)} = -\lambda_{m-1}^{(2m)}$, then the element of $\mathfrak{t}_{2m,+}^*$ we are denoting $\lambda^{(2m)}$ ends in the block $\beta(\lambda_{m-1}^{(2m)})^{\oplus d_{\ell-1}} \oplus \beta(-\lambda_{m-1}^{(2m)})$, which is the conjugate of $\beta(\lambda_{m-1}^{(2m)})^{\oplus d_{\ell}}$ by the permutation matrix $o = [1]^{\oplus d_{\ell}-2} \oplus \begin{bmatrix} 0 & 1 \\ 1 & 0 \end{bmatrix}$; it follows the corresponding block of H_k is the conjugate $\text{U}(d_{\ell})^o$.¹³ If we write U_{ℓ} for the ℓ^{th} block of H_k in all cases, then we have

$$H_k = \text{U}(d_1) \oplus \cdots \oplus \text{U}(d_{\ell-1}) \oplus \text{U}_{\ell} \oplus \text{SO}(d_0) \quad (2.3.10)$$

where $\text{SO}(1) \cong \text{SO}(0) := \{1\}$ and d_0 is always congruent to k modulo 2.

2.3.11 (Representatives $\zeta^{(k+1)}$ and groups L_k). The range of options for $\zeta^{(k+1)}$ in 2.1.6 for the orthogonal case is a variant of (2.2.8), with $\beta(\mu_i)^{\oplus d_i}$ replacing $\text{diag}(\mu_i, \dots, \mu_i)$ for $0 < i < \ell$, the o -conjugate replacing it for $i = \ell$, and an extra block of zeroes corresponding to the $\text{SO}(d_0)$ factor

¹³ Hence this block is not conjugate to $\text{U}(d_{\ell})$ in $\text{SO}(k)$ but becomes so in $\text{SO}(k+1)$. This dichotomy will not be reflected in the quotients H_k/L_k , but will affect our description of L_k and of the horizontal maps $G_k/L_k \rightarrow G_{k+1}/H_{k+1}$ in Figure 2.1.3.

of H_k . The z_i are replaced by arbitrary vectors in \mathbb{R}^{2d_i} or \mathbb{R}^{d_0} of fixed norm r_i , which continue to be continuous in $p \in \Delta$ and c by 0. We continue to take $z_i = [r_i \ 0 \ \cdots \ 0]^\top$ when possible and $z'_\ell = [0 \ \cdots \ 0 \ r_\ell]^\top$ when necessary. The standard choice of $\zeta^{(k+1)}$ has stabilizer

$$L_k = K_1 \oplus \cdots \oplus K_{\ell_k} \oplus K_0 \leq \mathrm{U}(d_1) \oplus \cdots \oplus \mathrm{U}_\ell \oplus \mathrm{SO}(d_0) = H_k, \quad (2.3.12)$$

where the blocks are given as follows, with the conventions $\mathrm{SO}(0) := \{1\} =: \mathrm{U}(0)$.

- For $1 \leq i < \ell$, and $i = \ell$ with $\mathrm{U}_\ell = \mathrm{U}(d_\ell)$, the K_i are as in the unitary case.
- If $\mathrm{U}_\ell = \mathrm{U}(d_\ell)^\circ$, then K_ℓ is U_ℓ for a \square -shape and $([1] \oplus \mathrm{U}(d_\ell - 1))^\circ$ for a \triangle -shape.
- The group K_0 is $\mathrm{SO}(d_0)$ for a ∇ - or \square -shape and $[1] \oplus \mathrm{SO}(d_0 - 1)$ for a \triangle -shape.

The alternative choice $'\zeta^{(k+1)}$ is again related to $\zeta^{(k+1)}$ by $'\zeta^{(k+1)} = \varphi_k(h)\zeta^{(k+1)}$ for some $h = \bigoplus_{i=1}^\ell u_i \oplus u_0 \in \bigoplus_{i=1}^{\ell-1} \mathrm{SU}(d_i) \oplus \mathrm{SU}_\ell \oplus \mathrm{SO}(d_0)$, where SU_ℓ is either $\mathrm{SU}(d_\ell)$ or $\mathrm{SU}(d_\ell)^\circ$.

Example 2.3.13. Consider the orthogonal GZ pattern in Figure 2.3.8. From rows 4 and 5 we see that $H_4 = \mathrm{U}(2) \times \mathrm{U}(2)$ and $L_4 = ([1] \oplus \mathrm{U}(1)) \times ([1] \oplus \mathrm{U}(1))$, from rows 3 and 4 we see that $H_3 = L_3 = \mathrm{U}(1) \times \mathrm{U}(1)$, and from rows 2 and 3 we see that $H_2 = \mathrm{SO}(2)$ and $L_2 = \{1\}$.

3. The structure of Gelfand–Zeitlin fibers

We begin in Section 3.1 by identifying a system of coordinates on $\Psi^{-1}(p)$ in $\prod G_k/L_k$ and connecting this to the staircase Figure 2.1.3. Unpacking this in Section 3.2 allows us to identify the horizontal maps in the diagram abstractly and to change them without altering the diffeomorphism type of the final pullback. In Section 3.3, we explicitly identify these maps in the cases of unitary and orthogonal Gelfand–Zeitlin systems. In Section 3.4, we rewrite the bundle towers of 2.1.6 as balanced products (Theorem 3.4.3); these are equivalent to biquotients (Proposition 3.4.13). A direct product decomposition of GZ fibers indexed by pattern components, follows immediately from this description (Corollary 3.5.1). Moreover, these factors generically simplify substantially (3.5.7, 3.5.19, 3.5.20). In Section 3.6, we derive a toral direct factor for both unitary and orthogonal GZ fibers in an elementary manner from the balanced product description and show the resulting torus action is the same given by the Thimm trick (Theorem 3.6.9). Interspersed throughout, we give a number of examples demonstrating these results. In particular, we recover Bouloc, Miranda, and Zung’s description of regular, elliptic, and (multi-)diamond fibers of unitary GZ systems as special cases.

3.1. Coordinate systems and transition functions

In this subsection, we are again in the general set-up of a topological Gelfand–Zeitlin system Ψ , as in Definition 2.1.1 and 2.1.6, trying again to characterize when a list of elements of $\prod_{k=\alpha}^n \Psi_k^{-1}(\lambda^{(k)})$ is the list of iterated Φ -images of some $\vartheta^{(n+1)} \in \Psi^{-1}(p)$.

3.1.1 (The staircase, G_k/L_k coordinates, and conjugating elements a_k). The staircase of Figure 2.1.3, interpreted through the lens of 2.1.6, represents $\Psi^{-1}(p) \cong F_\alpha^{n+1}$ as the iterated fiber product

$$G_\alpha/L_\alpha \times_{G_{\alpha+1}/H_{\alpha+1}} G_{\alpha+1}/L_{\alpha+1} \times_{G_{\alpha+2}/H_{\alpha+2}} \cdots \times_{G_n/H_n} G_n/L_n, \quad (3.1.2)$$

a subset of the direct product $\prod_{k=\alpha}^n G_k/L_k$ comprising certain lists $(g_k L_k)$.

What are these g_k ? Consider a point $\vartheta^{(n+1)} \in \Psi^{-1}(p)$ and recall that we fixed a choice of representatives $\zeta^{(k+1)} \in \mathcal{O}_{\lambda^{(k+1)}} \cap \Phi^{-1}(\lambda^{(k)}) = \mathcal{O}_{\lambda^{(k+1)}, \lambda^{(k)}}$. The transitivity condition along with the assumption that $\vartheta^{(n+1)}$ lies in $F_n^{n+1} = \mathcal{O}_{\lambda^{(n+1)}, \lambda^{(n)}}$ implies that $\varphi(g_n)\zeta^{(n+1)} = \vartheta^{(n+1)}$ for some $g_n \in G_n$. Similarly, that $\Phi(\vartheta^{(n+1)})$ lies in $F_{n-1}^n = \mathcal{O}_{\lambda^{(n)}, \lambda^{(n-1)}}$ implies there is some $g_{n-1} \in G_{n-1}$ with $\varphi(g_{n-1})\zeta^{(n)} = \Phi(\vartheta^{(n+1)})$ and so on, so that $(g_k L_k)$ corresponds to the list $(\varphi(g_k)\zeta^{(k+1)}) = (\Phi^{n+1-k}(\vartheta^{(n+1)}))$ of iterated truncations of $\vartheta^{(n+1)}$.

Which lists occur is determined by a set of coherence conditions involving the projections $G_k/L_k \longrightarrow G_k/H_k$ and the maps

$$G_k/L_k \xrightarrow{\sim} \varphi(G_k) \cdot \zeta_{k+1} \hookrightarrow G_{k+1} \cdot \lambda^{(k+1)} \xrightarrow{\sim} G_{k+1}/H_{k+1}$$

we now characterize.

Lemma 3.1.3. *Make identifications $F_k^k = \mathcal{O}_{\lambda^{(k+1)}, \lambda^{(k)}} \cong G_k/L_k$ and $F_k^{k+1} = \mathcal{O}_{\lambda^{(k+1)}} \cong G_{k+1}/H_{k+1}$ by fixing $\zeta^{(k+1)} \in \mathcal{O}_{\lambda^{(k+1)}, \lambda^{(k)}}$ and $\lambda^{(k+1)} \in \mathcal{O}_{\lambda^{(k+1)}}$ as in 2.1.6, and let $a_{k+1} \in G_{k+1}$ be such that $\lambda^{(k+1)} = a_{k+1}\zeta^{(k+1)}$. Then $F_k^{k+1} \longrightarrow F_{k+1}^{k+1}$ is identified with the map $G_k/L_k \longrightarrow G_{k+1}/H_{k+1}$ given by*

$$\iota_{a_{k+1}, 1}: gL_k \longmapsto \varphi_k(g)a_{k+1}^{-1}H_{k+1}. \quad (3.1.4)$$

3.1.5. The compatibility conditions for a point $(g_k L_k)$ to lie in the fiber product are then

$$\varphi(g_k)a_{k+1}^{-1}H_{k+1} = g_{k+1}H_{k+1} \quad (\alpha \leq k \leq n-1). \quad (3.1.6)$$

From a point in the fiber product (3.1.2), the element $\vartheta^{(n+1)} \in \mathcal{O}$ can be recovered again as $\varphi(g_n)\zeta^{(n+1)} = \varphi(g_n)a_{n+1}^{-1}\lambda^{(n+1)}$.¹⁴

3.1.7 (The effects of changing ζ). We fixed the representatives $\lambda^{(k)}$ and groups $H_k = \text{Stab}_{G_k} \lambda^{(k)}$ in 2.1.5 permanently, and chose $\zeta^{(k+1)}$ in 2.1.6 provisionally, with the warning in Remark 2.2.11 that we would later need to consider different choices. If change $\zeta^{(k+1)}$ to $'\zeta^{(k+1)} = \varphi_k(h)\zeta^{(k+1)}$ for some $h \in H_k/L_k$, fixing the other representatives, then in (3.1.2) and (3.1.6) we get

$$L'_k = hL_k h^{-1}, \quad g'_k = g_k h^{-1}, \quad a'_{k+1} = a_{k+1} \varphi_k(h)^{-1},$$

the other L_j, g_j , and a_j being unchanged.

3.2. A new pullback

Construction 3.2.1. We might consider changing $\iota_{a,1}$ in (3.1.4) to

$$\iota_{a,b}: gL_k \longmapsto b\varphi_k(g)a^{-1}H_k$$

for some $b \in G_{k+1}$. Since $\iota_{a,b}$ is equal to the composition of $\iota_{a,1}$ with left translation by b on G_{k+1}/H_{k+1} , which is an automorphism of the bundle $G_{k+1}/L_{k+1} \longrightarrow G_{k+1}/H_{k+1}$, the pullbacks of this bundle by $\iota_{a,b}$ and $\iota_{a,1}$ are diffeomorphic. It follows that the resulting final pullbacks $F_\alpha^{n+1} \cong \Psi^{-1}(p)$ in Figure 2.1.3 will be diffeomorphic if we make such a change for any number of k .

¹⁴ Since the horizontal maps in Figure 2.1.3 are all injections, the coordinates $g_k L_k$ for $k < n$ in some sense merely ensure that g_n satisfies the compatibility conditions.

In particular, we would like to instead take $b_{k+1} = a_{k+1}$ for all k , allowing us to reanalyze the horizontal maps in Figure 2.1.3 as composites

$$\frac{G_k}{L_k} \xrightarrow{\sim} \frac{a\varphi(G_k)a^{-1}}{a\varphi(L_k)a^{-1}} \longrightarrow \frac{G_{k+1}}{H_{k+1}}, \quad (3.2.2)$$

the first factor being induced by the map $c_a \circ \varphi: G_k \longrightarrow G_{k+1}$ taking g to $a\varphi(g)a^{-1}$ and the second by the inclusion.

Notation 3.2.3. We will write Ω_p^r for F_α^{n+1} in (3.1.2) under the maps $g_k L_k \longmapsto \varphi_k(g_k)a_{k+1}^{-1}H_{k+1}$ and Ω_p^c for the (diffeomorphic) pullback under the maps $g_k L_k \longmapsto a_{k+1}\varphi_k(g_k)a_{k+1}^{-1}H_{k+1}$.

3.2.4 (Coordinate conversion from Ω_p^r to Ω_p^c). When the maps $G_k/L_k \longrightarrow G_{k+1}/H_{k+1}$ are altered per Construction 3.2.1, the conditions on coset lists $(\hat{g}_k L_k) \in \prod G_k/L_k$ from 3.1.5 become instead

$$a_{k+1}\varphi_k(\hat{g}_k)a_{k+1}^{-1}H_{k+1} = \hat{g}_{k+1}H_{k+1} \quad (\alpha \leq k \leq n-1).$$

For any choice of $a_\alpha \in G_\alpha$ (of course, $a_\alpha = 1$ is most natural), and omitting the φ_k from the notation to make the pattern clearer, an explicit diffeomorphism is $(g_k L_k) \longmapsto (\hat{g}_k L_k)$ with

$$\hat{g}_\alpha = a_\alpha g_\alpha, \quad \hat{g}_{\alpha+1} = a_{\alpha+1} a_\alpha \cdot g_{\alpha+1}, \quad \dots, \quad \hat{g}_n = a_n \cdots a_\alpha \cdot g_n.$$

3.2.5. We actually have more latitude to adjust the horizontal maps in Figure 2.1.3 without changing the diffeomorphism type of F_α^{n+1} . Indeed, given any automorphism σ of G_{k+1} taking H_{k+1} to itself, we may exchange the map φ_k for $\sigma \circ \varphi_k$, changing the map of (3.2.2) to $g_k L_k \longmapsto \sigma(a\varphi_k(g)a^{-1})H_{k+1}$ and leaving the diffeomorphism type of the fiber unchanged.

3.3. Continuity of transition functions

Now that we have a description of the horizontal maps in Figure 2.1.3, we are able to say what the elements $a_{k+1} \in G_k$ are for unitary and orthogonal Gelfand–Zeitlin fibers and as a result to describe the maps $c_{a_{k+1}} \circ \varphi_k$ figuring in Lemma 3.1.3. It will be important to us later that, like our choice of elements $\vartheta^{(k+1)}$, the a_{k+1} can locally be chosen continuous in p , at least for unitary and orthogonal Gelfand–Zeitlin systems.

3.3.1. For a unitary GZ system, we claim a natural choice of matrices $a = a_{k+1}$ conjugating $\zeta = \zeta^{(k+1)}$ to $\lambda^{(k+1)}$ is continuous. Note that the assumed equation $\lambda^{(k+1)} = \text{Ad}_a^* \zeta = a\zeta a^{-1}$, rearranged to $\zeta a^{-1} = a^{-1}\lambda^{(k+1)}$, means precisely that the j^{th} column of $a^{-1} = \bar{a}^\top$ lies in the $\lambda_j^{(k+1)}$ -eigenspace of ζ . Hence, to define a , it will be enough to find an orthonormal frame of such eigenvectors. Every instance of an eigenvalue of $\lambda^{(k)}$ also occurring as an eigenvalue of $\lambda^{(k+1)}$, say $\lambda_j^{(k+1)}$, corresponds to a j^{th} row of the “boring” form $\lambda_j^{(k+1)} \cdot (\delta^j)^\top = [0 \cdots 0 \lambda_j^{(k+1)} 0 \cdots 0]^\top$ in ζ , so we may take the column vector δ^j the j^{th} column of a^{-1} . If the corresponding component in the k^{th} and $(k+1)^{\text{st}}$ rows of the GZ pattern is a \square - or \triangle -shape, then we have found a basis for the corresponding eigenspace. Otherwise, in the case of a ∇ -shape, we have selected all but one basis eigenvector and the orthogonal complement to the others within the $\lambda_j^{(k)}$ -eigenspace of ζ is 1-dimensional, and so contains precisely a circle of candidate eigenvectors. From our convention for choosing the z_i in (2.2.8) to have only first coordinate nonzero, it will be the first column vector in a^{-1} (counting from the left) in the $\lambda_j^{(k)}$ -eigenspace of ζ that has this non- δ^j form.

Obviously the δ^j are continuous in ξ and orthonormal, but it could *a priori* be that the new w^{th} columns $v_w = [v_w^1 \cdots v_w^{k+1}]^\top$, which we only specified up to a constant in $U(1)$, cannot be continuously defined. To see they can be, note that the entries v_w^j for which the j^{th} row of ξ is $\lambda_j^{(k+1)} \cdot \delta^j$ must be 0 for v_w to be orthogonal to the columns $v_j = \delta^j$ we have already chosen. For the remaining j , the i^{th} row of ξ has the “interesting” form $[0 \cdots 0 \mu_i 0 \cdots 0 r_i]$. Multiplying the j^{th} row of ξ with the w^{th} column v_w of a^{-1} we are determining, which we assume is a $\lambda_w^{(k+1)}$ -eigenvector of ξ , we find the constraint $v_w^j = r_i (\lambda_w^{(k+1)} - \mu_i)^{-1} \cdot v_w^{k+1}$, meaning the other nonzero entries are uniquely determined as real multiples of the bottom entry v_w^{k+1} . Temporarily set this to 1 and call the resulting vector v'_w . Since $R = 1^2 + \sum_m (r_i / (\lambda_w^{(k+1)} - \mu_m))^2$ is a continuous function of ξ (here the sum is over interesting rows of ξ , corresponding to Δ -shapes), the vector $v_w = \frac{1}{\sqrt{R}} v'_w$ is a continuous function of ξ as well. The matrix a' is actually orthogonal, having only real entries. In case $\det a' = -1$, we can get a special orthogonal matrix b instead by substituting the last column v_{k+1} with $-v_{k+1}$. Finally, set $a = b^{-1}$.

We will later need to show that the elements $\xi^{(k+1)}$ and hence the elements a_{k+1} can also be chosen so as to be continuous over the union $E \cup F$ of the interior $E \subseteq \Delta$ of a face and that of an adjoining codimension-one face. To see this, we work matrix coefficient by matrix coefficient in (2.2.8). Most entries of $\xi^{(k+1)}$ are simply 0, which is surely continuous. Along the first k entries of the diagonal, we have convergence by assumption, since these entries are $\lambda^{(k)}(q)$. The last diagonal entry $c(q) = \text{tr} \lambda^{(k+1)}(q) - \text{tr} \lambda^{(k)}(q)$ is hence also continuous.

The remaining entries, r_i in the discussion in 2.2.7, yield to a case analysis. For r_i corresponding to a Δ -shape not labeled by μ^\pm , the expression (2.2.10) has $r_i(q) \rightarrow r_i(p)$ as $q \rightarrow p$ since we have $\mu^\pm \rightarrow \mu$ and no factor approaching 0 appears in denominator. For r_i corresponding to a Δ -shape labeled by μ^\pm , we subdivide by case. For $\square\square$ and $\square\nabla$, and symmetrically $\square\square$ and $\square\square$, there are no such r_i . For $\Delta\square$, μ^+ does not appear in (2.2.10) and $r_i(q) \rightarrow r_i(p)$ since $\mu^- \rightarrow \mu$. For $\square\Delta$, symmetrically, we use $'\xi^{(k+1)}$ in place of $\xi^{(k+1)}$ and again $r_i \rightarrow 0$, this time since $\mu^+ \rightarrow \mu$. For $\Delta\nabla$ the square $r_i(q)^2$ factors as a rational function of μ^- alone and the factor $\mu^- - \mu^+ \rightarrow 0$, so indeed $r_i(q) \rightarrow 0 = r_i(p)$. For $\nabla\Delta$, we take $'\xi^{(k+1)}(q)$ as noted above, and the discussion of r_i is the same as for $\Delta\nabla$.

The description and continuity of the $\xi^{(k+1)}$ are analogous in the orthogonal case, but more notationally involved.

3.3.2. In the unitary case, the map $c_a \circ \varphi: L_k \rightarrow H_{k+1}$ of (3.2.2) sends the factor K_j of L_k associated to the j^{th} connected component of the k^{th} row to the unitary factor $U(e)$ of H_{k+1} corresponding to the same connected component of the GZ pattern. In the case of a Δ - or \square -shape ($e = \text{rk } K_j = d_j - 1$ or d_j , respectively) the composite map $K_j \hookrightarrow L_k \xrightarrow{c_a} H_{k+1} \rightarrow U(e)$ is the natural isomorphism, respectively $[1] \oplus U(e) \xrightarrow{\sim} U(e)$ or $U(e) \xrightarrow{\cong} U(e)$. In the case of a ∇ -pattern ($e = d_j + 1$), this composition is the block-inclusion $[1] \oplus U(d_j) \hookrightarrow U(1 + d_j)$. Note that although the element a and hence the automorphism $c_a \in \text{Aut } G_{k+1}$ vary with p , the map $c_a \circ \varphi: L_k \rightarrow H_{k+1}$ as just described is the same for any two points in the interior of the same face of Δ .

3.3.3. Again in the orthogonal case, the map $c_a \circ \varphi: L_k \rightarrow H_{k+1}$ of (3.2.2) sends the factor K_j of L_k associated to the j^{th} connected component of the k^{th} row to the factor of H_{k+1} corresponding to the same connected component of the GZ pattern. For the white component, these factor inclusions $\text{SO}(d_0) \hookrightarrow L_k \xrightarrow{c_a} H_{k+1} \rightarrow \text{SO}(e)$ are as expected by analogy with the unitary case, either the identity map in the case of a Δ - or \square -shape, and $\text{SO}(d_0) \xrightarrow{\sim} [1] \oplus \text{SO}(d_0) \hookrightarrow \text{SO}(1 + d_0)$ in the case of a ∇ -shape.

The numerology of the inclusions $U(d) \hookrightarrow L_k \hookrightarrow H_{k+1} \twoheadrightarrow U(e)$ of unitary factors indexed by the same λ is the same as in the unitary case described in 3.3.2, with the same dependence on Δ -, \square -, or ∇ -shapes occurring in the GZ pattern, but the embeddings themselves may be different. The embeddings between *standardly embedded* unitary factors are the standard embeddings, as in that section.

By contrast, the embedding of a nonstandard unitary factor K_ℓ in a standard unitary factor $U(e)$ of H_{k+1} is given by $o^{-1}U(e)o \xrightarrow{c_o} U(e)$ in the cases of both a \square -shape and a Δ -shape (and a ∇ -shape cannot occur). The embedding of a standard K_ℓ in a nonstandard factor of H_{k+1} (necessarily $K_\ell = U(d_\ell)$ in this case since a Δ -shape cannot occur) is given by $U(d_\ell) \xrightarrow{c_o} U(d_\ell)$ for a \square -shape, but for a ∇ -shape is given by $U(d_\ell) \xrightarrow{\sim} U(d_\ell) \oplus [1] \hookrightarrow U(d_\ell + 1)^o$. Note that unlike in all other cases, this is an *upper-left* rather than lower-right block inclusion, and that the image is invariant under conjugation by o , which is equal to the identity matrix except in the lower-right 2×2 block. To deal with this case, we employ 3.2.5 to modify the map $G_k/L_k \rightarrow G_{k+1}/H_{k+1}$ by an automorphism σ of G_k preserving H_k . In this case, we let σ be conjugation by $o^{-1}Po$, where P is the matrix inducing the permutation exchanging the upper-left $2d_\ell \times 2d_\ell$ with the lower-right 2×2 submatrix. The factor in the replaced H_{k+1} is again $U(d_\ell + 1)^o$, and the injection from $K_\ell = U(d_\ell)$ is now $U(d_\ell) \xrightarrow{\sim} [1] \oplus U(d_\ell) \hookrightarrow U(1 + d_\ell)$ followed by c_o .

Note again that the restriction of the maps $c_a \circ \varphi$ or $\sigma \circ c_a \circ \varphi$ to L_k is the same for every p in the interior of a face of Δ even though the conjugating elements a vary from point to point.

3.4. Iterated balanced products and biquotients

It is in this section we undergo the perspective shift that we have claimed will simplify our lives. We begin with a straightforward lemma.

Definition 3.4.1. Suppose a group G acts on the right on a space X and on the left on a space Y . In this case, we define the *balanced product* $X \otimes_G Y$ to be the quotient $(X \times Y)/G$ under the diagonal action. The elements of $X \otimes_G Y$, which we denote $x \otimes y$, satisfy $xg \otimes y = x \otimes gy$.

Lemma 3.4.2. Let $\varphi: G \rightarrow \tilde{G}$ be a map of topological groups and let $L \leq G$ and $\tilde{L} \leq \tilde{H} \leq \tilde{G}$ be closed subgroups such that $\varphi(L) \leq \tilde{H}$. Suppose \tilde{L} acts continuously on a topological space X . Then the map

$$\begin{aligned} \varkappa: G/L \times_{\tilde{G}/\tilde{H}} \tilde{G} \otimes_{\tilde{L}} X &\longrightarrow G \otimes_L \tilde{H} \otimes_{\tilde{L}} X, \\ (gL, \tilde{g} \otimes x) &\longmapsto g \otimes \varphi(g)^{-1} \tilde{g} \otimes x, \end{aligned}$$

is a well-defined homeomorphism. If the homomorphisms are of compact Lie groups and X is a smooth manifold with smooth \tilde{L} -action, then \varkappa is a diffeomorphism.

Proof. Since the fiber product $G \times_{\tilde{G}/\tilde{H}} \tilde{G}$ is the set of pairs $(g, \tilde{g}) \in G \times \tilde{G}$ such that $\varphi(g)^{-1} \tilde{g}$ lies in \tilde{H} , the assignments $(g, \tilde{g}) \mapsto (g, \varphi(g)^{-1} \tilde{g})$ and $(g, h) \mapsto (g, \varphi(g)h)$ define a continuous map $G \times_{\tilde{G}/\tilde{H}} \tilde{G} \rightarrow G \times \tilde{H}$ and its continuous inverse. One checks using coset representatives that these descend to well-defined maps $\kappa: G/L \times_{\tilde{G}/\tilde{H}} \tilde{G} \rightarrow G \otimes_L \tilde{H}$ and κ^{-1} , necessarily homeomorphisms, and then that $\kappa \times \text{id}_X$ and $\kappa^{-1} \times \text{id}_X$ descend to a well-defined \varkappa and \varkappa^{-1} . Under the smoothness hypotheses, the original homeomorphism and its inverse are smooth, and as all the actions in question are free and proper, so the orbit spaces are again smooth manifolds and the quotient maps are smooth submersions, meaning \varkappa and \varkappa^{-1} are smooth as well. \square

Here, then, is the perspective shift.

Theorem 3.4.3. *Let Ψ be a topological Gelfand–Zeitlin system, $p \in \Delta$ a point, $L_k \leq H_k \leq G_k$ the groups discussed in 2.1.6, and a_{k+1} for $\alpha + 1 \leq k \leq n + 1$ elements as discussed in 3.1.1. Then there is a diffeomorphism between $\Psi^{-1}(p)$ and*

$$T_p := G_\alpha \otimes_{L_\alpha} H_{\alpha+1} \otimes_{L_{\alpha+1}} \cdots \otimes_{L_{n-1}} H_n / L_n$$

where the balanced products with respect to the groups L_k are taken with respect to the natural inclusion of L_k into H_k and the embedding of L_k into H_{k+1} via the homomorphism $c_{a_{k+1}} \circ \varphi_k$.

In both the orthogonal and unitary cases, we have $G_\alpha = H_\alpha$, so that in fact G_k does not figure.

Proof. We have a diffeomorphism $\Psi^{-1}(p) \xrightarrow{\sim} \Omega_p^r$ by 2.1.5 and a diffeomorphism $\Omega_p^r \rightarrow \Omega_p^c$ by Construction 3.2.1. Consider 2.1.3, with the horizontal maps induced by $c_{a_{k+1}}$ as discussed in Construction 3.2.1, so that $\Omega_p^c = F_\alpha^{n+1}$. We will prove diffeomorphisms

$$F_j^k \cong G_j \otimes_{L_j} H_{j+1} \otimes_{L_{j+1}} \cdots \otimes_{L_{k-2}} H_{k-1} \otimes_{L_{k-1}} *, \quad (\alpha \leq j < k \leq n + 1)$$

so the result will follow on taking $j = \alpha$ and $k = n + 1$. For any fixed vertical index k , the claim is proved by decreasing (i.e., leftward) induction on the horizontal index j . For the base case, when $j = k - 1$, the expression simplifies to $F_{k-1}^k \cong G_{k-1} / L_{k-1}$. For the induction step, assume the diffeomorphism for j and consider the tall rectangle $F_{[j-1, j]}^{[j, k]}$ comprising $k - j$ vertically stacked boxes in (2.1.3). We have $F_{j-1}^j = G_{j-1} / L_{j-1}$ and $F_j^j = G_j / H_j$, and by induction an expression $G_j \otimes_{L_j} X$ for F_j^k . For this X and $(G, L) = (G_{j-1}, L_{j-1})$ and $(\tilde{G}, \tilde{H}, \tilde{L}) = (G_j, H_j, L_j)$, an application of Lemma 3.4.2 completes the induction. \square

Since the groups H_k and L_k depend only on the face of Δ containing p in its interior, we recover in arguably more explicit form Cho–Kim–Oh’s observation that the diffeomorphism type of a Gelfand–Zeitlin fiber $\Psi^{-1}(p)$ is determined entirely by the open face of Δ containing p .

3.4.4 (Coordinate conversion from Ω_p^c to T_p). An inductive calculation shows the diffeomorphism $\Omega_p^c \rightarrow T_p$ takes $(\hat{g}_k L_k)$ to

$$\hat{g}_\alpha \otimes (c_{a_{\alpha+1}} \circ \varphi_\alpha)(\hat{g}_\alpha)^{-1} \cdot \hat{g}_{\alpha+1} \otimes (c_{a_{\alpha+2}} \circ \varphi_{\alpha+1})(\hat{g}_{\alpha+1})^{-1} \cdot \hat{g}_{\alpha+2} \otimes \cdots \otimes (c_{a_n} \circ \varphi_{n-1})(\hat{g}_{n-1})^{-1} \cdot \hat{g}_n L_n. \quad (3.4.5)$$

It follows that starting with a point $\varphi_n(g_n)\zeta^{(n)} = \varphi_n(g_n)a_{n+1}^{-1}\lambda^{(n+1)}$ of $\mathcal{O}_{\lambda^{(n+1)}}$, converting it to the point $(g_k L_k) \in \Omega_p^r$, converting this in turn to the point $(\hat{g}_k L_k) \in \Omega_p^c$ via 3.2.4, and then finally converting to a point of T_p , one recovers the point

$$g_\alpha \otimes a_{\alpha+1} \varphi_\alpha(g_\alpha)^{-1} g_{\alpha+1} \otimes a_{\alpha+2} \varphi_{\alpha+1}(g_{\alpha+1})^{-1} g_{\alpha+2} \otimes \cdots \otimes a_n \varphi_{n-1}(g_{n-1})^{-1} g_n L_n \in T_p. \quad (3.4.6)$$

Although the elements $a_{k+1}(p) \in G_{k+1}$ continuously vary, in Proposition 3.5.6, we fixed p and then explicitly identified in 3.3.2 and 3.3.3 the effect of the conjugation maps $L_k \rightarrow H_{k+1}$ on block components, and found that for our standard choice of $\zeta^{(k+1)}$ they were block inclusions of a standard form. Since we had fixed p before this discussion found that these injections were of this form, they are actually independent of p . It follows that the description of T_p in Theorem 3.4.3 does not depend on the choice of representatives $\zeta^{(k+1)}$ and within the interior of any given face of Δ , does not depend on p either. The same follows for the map $\Omega_p^c \rightarrow T_p$ of (3.4.5). We will discuss in Section 4.3 how much this changes in transitioning between faces.

3.4.7 (The effects on T_p of changing ξ). On the other hand, the diffeomorphism $\Omega_p^r \rightarrow T_p$ does depend on p because the values a_k appear once each in (3.4.6). Indeed, in 3.1.7, we discussed the effects of a change of ξ_{k+1} to $\varphi(h)\xi_{k+1}$ in the description of Ω_p^r . Applying 3.4.4, owing to cancellation of the new h 's in g'_k and a'_{k+1} , in the balanced product representation, the point in (3.4.6) then becomes

$$g_\alpha \otimes \cdots \otimes a_k \varphi_{k-1}(g_{k-1})^{-1} g_k h^{-1} \otimes \cdots \otimes a_n \varphi_{n-1}(g_{n-1})^{-1} g_n L_n \in T_p, \quad (3.4.8)$$

with only the displayed k^{th} tensor-coordinate changed. In particular, the balanced product presentation of Theorem 3.4.3 does depend on the choice of orbit representatives $\xi^{(k+1)}$.

Remark 3.4.9. Interestingly, Bouloc–Miranda–Zung [BouMZ18, Thm. 4.16] obtain a different description of a GZ fiber as a biquotient. We know only special cases where their expressions and ours simplify to the same thing (Examples 3.5.12 and 3.5.14).

Remark 3.4.10. Another instance of the balanced iterated product construction is the *generalized Bott towers* of Kaji, Kuroki, Lee, and Suh [KaKLS20, Defs. 3.1, 3.5]. Inspecting cohomology, one sees a generalized Bott tower is almost never a GZ fiber.

Remark 3.4.11. This sort of iterated balanced product can be expressed perhaps less usefully as a two-sided quotient.

Definition 3.4.12. When A and B are closed subgroups of a Lie group G such that the action $(a, b) \cdot g := agb^{-1}$ of $A \times B$ on G is free, the orbit space is called a *biquotient* and denoted $A \backslash G / B$.

Proposition 3.4.13 (Biquotient description). *The expression T_p of Theorem 3.4.3 is diffeomorphic to a biquotient of Lie groups. Explicitly, let*

$$\begin{aligned} G &= \prod_{k=1}^n H_k, \\ A &= \{(1, \ell_2, \ell_2, \ell_4, \ell_4, \dots) \in G : \ell_{2i} \in L_{2i}\}, \\ B &= \{(\ell_1, \ell_1, \ell_3, \ell_3, \dots) \in G : \ell_{2i-1} \in L_{2i-1}\}, \end{aligned} \quad (3.4.14)$$

where we have suppressed the maps φ_k for legibility. Then a diffeomorphism $A \backslash G / B \rightarrow T_p$ is given by

$$A(g_1, g_2, g_3, g_4, \dots)B \mapsto g_1 \otimes g_2^{-1} \otimes g_3 \otimes g_4^{-1} \otimes \cdots \otimes g_n^{(-1)^n} L_n.$$

3.5. Diagram components, direct factors, and simplifications

We now explain how the expression T_p of Theorem 3.4.3 can be simplified: it factors and those factors tend to telescope. Afterwards we will give several concrete examples.

Corollary 3.5.1. *Every unitary or orthogonal Gelfand–Zeitlin fiber is diffeomorphic to a direct product of factors indexed by certain connected components of the pattern. For a unitary GZ pattern, each component contributes one factor. For an orthogonal GZ pattern, each component of the positive part and each white component contributes one direct factor.*

Proof. By Theorem 3.4.3, $\Psi^{-1}(p)$ is diffeomorphic to the iterated balanced product T_p . The groups L_k and H_k decompose into direct products of factors which correspond to connected components of the k^{th} row of the GZ pattern. (2.2.6) and (2.3.10) show the inclusions $L_k \rightarrow H_k$ send each block of L_k into the block of H_k corresponding to the same component of the GZ pattern, and (2.2.9) and (2.3.12) show the same for the injections $c_{a_{k+1}} \circ \varphi_k : L_k \rightarrow H_{k+1}$. Now observe that given an indexed list $M_j \leftarrow K_j \rightarrow N_j$ of diagrams of groups, one has $\prod M_j \otimes_{\prod K_j} \prod N_j \cong \prod (M_j \otimes_{K_j} N_j)$. \square

Notation 3.5.2. In the product decomposition of an orthogonal GZ fiber given by Corollary 3.5.1, we write F_U for the product of the factors corresponding to white components in the corresponding Gelfand–Zeitlin pattern and F_{SO} for the product of the factors corresponding to white components. Hence $F \cong F_U \times F_{SO}$.

3.5.3 (The two types of direct factor). It is often possible to obtain much more concise expressions for the factors described in Corollary 3.5.1. Suppose we are given a connected component of a GZ pattern (unitary or orthogonal) beginning in row k_b and ending in row k_t . For any integer $k \in [k_b, k_t]$, write $w(k)$ for the *width* of row k of the component, i.e., the number of vertices in the component in this row. The width $w(k_b)$ of the bottom row in the connected component is always 1, and $w(k_t)$ is also 1 unless $k_t = n + 1$, meaning the component ends in the top row of the GZ pattern. There are two different cases to analyze, depending whether or not $k_t < n + 1$.

If $k_t \leq n$, then the direct factor corresponding to the given connected component is of the form

$$J_{k_b} \otimes_{K_{k_b}} J_{k_b+1} \otimes_{K_{k_b+1}} \cdots \otimes_{K_{k_t-2}} J_{k_t-1} \otimes_{K_{k_t-1}} J_{k_t} \quad (3.5.4)$$

where the factors $K_k \leq J_k$ for $k_b \leq k \leq k_t$ are the factors of L_k and H_k (respectively) described by (2.2.6) and (2.2.9) in the unitary case and (2.3.10) and (2.3.12) in the orthogonal case. Note that K_{k_t} is trivial since $k_t \leq n$. For a black component (one of a pair, in the orthogonal case), we have $J_k \cong U(w(k))$, and for a white component, we have $J_k \cong SO(w(k))$. On the other hand, if $k_t = n + 1$, there is no group J_{n+1} , and the factor corresponding to the given connected component has the form

$$J_{k_b} \otimes_{K_{k_b}} J_{k_b+1} \otimes_{K_{k_b+1}} \cdots \otimes_{K_{n-1}} J_n/K_n. \quad (3.5.5)$$

Proposition 3.5.6. *In the case of a unitary Gelfand–Zeitlin pattern, the groups J_k and K_k in the above descriptions may be taken to be unitary groups and each inclusion $J_k \rightarrow K_k$ and $J_k \rightarrow K_{k+1}$ can be taken to be the identity or a lower-right block inclusion $U(d) \xrightarrow{\sim} [1] \oplus U(d) \hookrightarrow U(1+d)$. In the case of an orthogonal Gelfand–Zeitlin pattern, the same holds for each factor of F_U , and for a factor of F_{SO} , the inclusions can each be taken to be the identity or of the form $SO(d) \xrightarrow{\sim} [1] \oplus SO(d) \hookrightarrow SO(1+d)$.*

Proof. For the case of a unitary GZ fiber, this follows immediately from our description of the groups H_k and L_k and the maps $c_a \circ \varphi: L_k \rightarrow H_{k+1}$. In the orthogonal case, The description is similarly immediate for F_{SO} and components of F_U in which all J_k and K_k are standard unitary.

The argument for components with any nonstandard unitary J_k is more involved. We observe an iterated balanced product as in (3.5.4) or (3.5.5) is determined by a zig-zag diagram

$$J_{k_b} \longleftarrow K_{k_b} \longrightarrow J_{k_b+1} \longleftarrow K_{k_b+1} \longrightarrow \cdots \longleftarrow K_{k_t-1} \longrightarrow J_{k_t} \longleftarrow K_{k_t},$$

where $K_{k_t} = 1$ unless $t = n + 1$, and that an isomorphism of such diagrams, meaning a sequence of Lie group isomorphisms $J_k \xrightarrow{\sim} J'_k$ and $K_k \xrightarrow{\sim} K'_k$ connecting such a zig-zag with another in such a way that all squares commute, induces a diffeomorphism of the one iterated balanced product with the other.

Now if k is even and $J_k = U(d)^o$ is nonstandard, our description of H_k , L_k , and $c_A: L_{k-1} \rightarrow H_k$ tells us the following. First, K_k is again $U(d)^o$ or is $([1] \oplus U(d-1))^o$; let us agree to write $U(e)^o$ for either. The unitary group $J_{k+1} \cong K_k$ is standard, with the map $K_k \rightarrow J_{k+1} = U(e)$ an isomorphism given by conjugation c_o by the transposition matrix o . Following our modification of the map $K_{k-1} \rightarrow J_k$, there are two possibilities for K_{k-1} , either $U(d)$ or $U(d-1)$, and the map is given by

either the identity or the lower-right block inclusion into $U(d)$, followed in both cases by c_o . Let us agree to write $K_{k-1} = U(f)$ in either case and write i for the inclusion $U(f) \rightarrow U(d)$, which may be the identity. Then we have the following isomorphism of zig-zags:

$$\begin{array}{ccccccc} \cdots & \longleftarrow & U(f) & \xrightarrow{c_o \circ i} & U(d)^o & \longleftarrow & U(e)^o & \xrightarrow{c_o} & U(e) & \longleftarrow & \cdots \\ & & \downarrow = & & \downarrow c_o & & \downarrow c_o & & \downarrow = & & \\ \cdots & \longleftarrow & U(f) & \xrightarrow{i} & U(d) & \longleftarrow & U(e) & \xrightarrow{=} & U(e) & \longleftarrow & \cdots, \end{array}$$

where the maps not displayed are the identity, and the displayed part of the bottom zig-zag is standard. Applying one of these isomorphisms for each nonstandard J_k , we arrive at a zig-zag where all J_k and K_k are standard unitary, and all maps $K_k \rightarrow J_{k+1}$ are the identity or the inclusion of $U(d)$ in $U(d+1)$ as the lower-right block. \square

3.5.7 (Telescopy). We may further simplify the expression (3.5.4) as follows. For each integer $k \in [k_b, k_t - 1]$, the expression contains a factor $J_k \otimes_{K_k} J_{k+1}$ determined by the pair of consecutive rows $k, k+1$. When these rows form an Δ -shape or a \square -shape, then $K_k = J_{k+1}$ so we have the simplification $J_k \otimes_{K_k} J_{k+1} \cong J_k$, whereas if they form a ∇ -shape, then $K_k = J_k$, so we have $J_k \otimes_{K_k} J_{k+1} \cong J_{k+1}$. Iterating the procedure, one can always simplify the expression (3.5.4) into one of the following forms.

First assume $k_t \leq n$, meaning the corresponding GZ pattern component ends before the top row. If each row is of width 1, then the expression collapses to one factor, $U(1)$ for a black component or $SO(1) = *$ for a white component. Otherwise, take a subsequence

$$\tilde{\ell}_1 \leq \ell_1 \leq \tilde{\ell}_2 \leq \ell_2 \leq \cdots \leq \tilde{\ell}_{r-1} \leq \ell_{r-1} \leq \tilde{\ell}_r,$$

of $[k_b + 1, k_t - 1]$ such that $M_i = w(\tilde{\ell}_i)$ and $m_i = w(\ell_i)$ are, respectively, the sequences of local maximum and minimum values of the function w on the interval $[k_b, k_t]$. Then the expression (3.5.4) telescopes to $J_{\tilde{\ell}_1} \otimes_{K_{\ell_1}} J_{\tilde{\ell}_2} \otimes_{K_{\ell_2}} \cdots \otimes_{K_{\ell_{r-1}}} J_{\tilde{\ell}_r}$, which is

$$U(M_1) \otimes_{U(m_1)} \cdots \otimes_{U(m_{r-1})} U(M_r) \quad \text{or} \quad SO(M_1) \otimes_{SO(m_1)} \cdots \otimes_{SO(m_{r-1})} SO(M_r) \quad (3.5.8)$$

depending on whether the component is black or white. In the case of a white component, this expression corresponds to a decomposition of the component into maximal hexagons and pentagons.

The analysis in the $k_t = n + 1$ expression is similar. In the degenerate case where each row is of width 1, the expression collapses to $U(1)/U(1)$ or $SO(1)/SO(1)$, which is a point either way. Otherwise, much as before, the expression (3.5.5) telescopes to $J_{\tilde{\ell}_1} \otimes_{K_{\ell_1}} J_{\tilde{\ell}_2} \otimes_{K_{\ell_2}} \cdots \otimes_{K_{\ell_{r-1}}} J_{\tilde{\ell}_r}/K_n$. More explicitly, depending on whether it is a black or white component respectively, this equals

$$U(M_1) \otimes_{U(m_1)} \cdots \otimes_{U(m_{r-1})} U(M_r)/K_n \quad \text{or} \quad SO(M_1) \otimes_{SO(m_1)} \cdots \otimes_{SO(m_{r-1})} SO(M_r)/K_n \quad (3.5.9)$$

where $M_i = w(\tilde{\ell}_i)$ and $m_i = w(\ell_i)$ as before. The group K_n is determined by the shape that occurs in the connected component between the top two rows (see examples below).

3.5.10 (Stiefel bundles). It will be useful later that (3.5.4) and (3.5.5) give an iterated fiber bundle construction for each of the direct factors described in Corollary 3.5.1, with base $J_{\tilde{\ell}_1}/K_{\ell_1}$ and

fibers $J_{\tilde{\ell}_i}/K_{\ell_i}$ and either $J_{\tilde{\ell}_r}/K_n$ or $J_{\tilde{\ell}_r}$. Similarly, (3.5.8) and (3.5.9) give another iterated fiber bundle construction for the direct factors, with base $U(M_1)/U(m_1)$ or $SO(M_1)/SU(m_1)$ and fibers $U(M_j)/U(m_j)$ or $SO(M_j)/SO(m_j)$ or $U(M_r)$ or $SO(M_r)$. These are all complex Stiefel manifolds $V_{M-m}(\mathbb{C}^M) = U(M)/U(m)$ or real Stiefel manifolds $V_{M-m}(\mathbb{R}^M) = SO(M)/SO(m)$ (with $m = 0$ recovering $U(M)$ and $m \in \{0, 1\}$, $SO(M)$). Stiefel manifolds are themselves interpretable as iterated sphere bundles over spheres using $U(k+1)/U(k) \cong S^{2k+1}$ and $SO(k+1)/SO(k) \cong S^k$, so this iterated bundle description gives a refinement of the existing iterated sphere bundle descriptions of Cho–Kim–Oh and Cho–Kim [CKO20, CK20].

Remark 3.5.11. One might hope therefore that the cohomology ring of a GZ fiber should agree with that of the product of the iterated Stiefel fibers. In Theorem 5.2.1 we will show this is true of unitary GZ fibers. For orthogonal GZ fibers, we will see in Theorem 5.3.12 that this is true over $\mathbb{Z}[1/2]$ and for the cohomology groups over \mathbb{Z} , but we find in Example 5.3.18 that it is not true for the cohomology ring over \mathbb{Z} .

Example 3.5.12 (Diamonds in unitary GZ patterns). Suppose that a connected component of a unitary GZ pattern is such that the sequence of local minimum and maximum widths, omitting first and last rows, contains a single entry (necessarily a local maximum, with $w \geq 2$). If the component ends before the top row, the corresponding direct factor is $U(w)$. If it ends in the top row, the corresponding factor is $U(w)/U(1) \cong SU(w)$. In the special case where the sequence of widths strictly increases to w and strictly decreases afterward, this recovers the existing description of “diamond singularities” [BouMZ18, §5(e)].

Example 3.5.13 (Diamonds in orthogonal GZ patterns). Suppose a white connected component of an orthogonal GZ pattern is a diamond of width $w \geq 2$, i.e., the sequence of local minimum and maximum widths increases to w and then decreases to 1, as in Figure 3.5.17b or Figure 3.5.17a. Then the corresponding direct product factor is $SO(w)$.

Example 3.5.14 (Torus fibers in unitary GZ systems). As noted above, a connected component of a unitary GZ pattern that has maximum width equal to 1 and ends below the top row contributes a factor of $U(1)$, i.e., a circle. A connected component ending in the top row and with $w(k)$ nondecreasing contributes $U(w(n))/U(w(n))$, i.e., a point. In particular, a unitary GZ fiber is a torus if and only if all the connected components of the associated GZ pattern have one of these forms, and in this case, the dimension of the torus is the number of connected components not connected to the top row. This recovers the description of “elliptic non-degenerate singular fibers” given by Bouloc *et al.* [BouMZ18, §5(c)]. These are not the only circle factors in general, as we discuss in Section 3.6.

Example 3.5.15 (Torus fibers in orthogonal GZ systems). We can similarly characterize toral factors of an orthogonal GZ fiber contributed by factors corresponding to white components of the pattern, as follows. A white connected component consisting of an isolated vertex contributes a point. A white diamond of width 2 (i.e., a white connected component consisting of three rows with widths 1, 2, 1) contributes $SO(2)/SO(1)$, i.e., a circle. A white connected component ending in the top row and with $w(k)$ nondecreasing contributes a point. An orthogonal GZ fiber is a torus if and only if all the white components have one of these forms and all the black components have one of the forms from Example 3.5.14.

Example 3.5.16. Consider the orthogonal GZ pattern in Figure 2.3.8. The black diamond in the positive part contributes a factor of $U(2)/U(1) \cong SU(2)$ and the white diamond of width 2 contributes a factor of $SO(2)$. Thus the GZ fiber is diffeomorphic to $SU(2) \times SO(2)$.

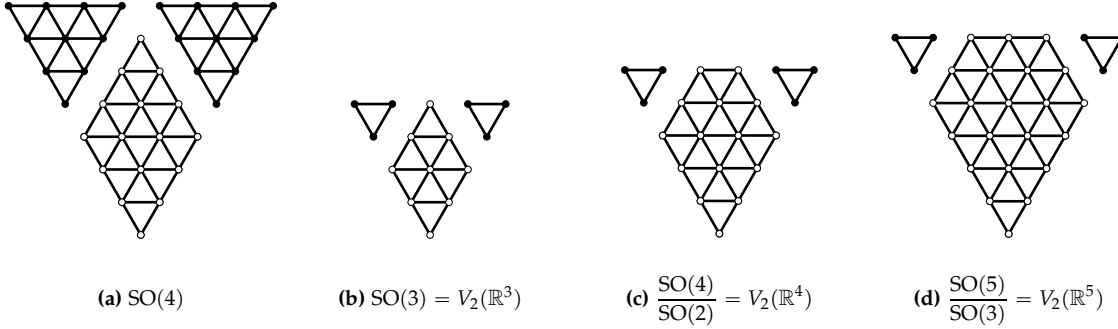


Figure 3.5.17: Some orthogonal Gelfand–Zeitlin patterns

It will be important to our later analysis that all connected real and complex Stiefel manifolds (i.e., all but $O(n)$) can be realized as GZ fibers.

Example 3.5.18 (Stiefel manifolds). Suppose a connected component of a GZ pattern contains vertices in the top row and the sequence of widths weakly increases from 1 to $w = w(\ell)$ and thereafter weakly decreases to $v = k(n+1)$ (for instance the component could be a pentagon), as in Figures 3.5.17c and 3.5.17d. Then the corresponding direct factor is the complex Stiefel manifold $V_{w-v}(\mathbb{C}^w) \cong U(w)/U(v)$ if the component is black, and the real Stiefel manifold $V_{w-v}(\mathbb{R}^w) \cong O(w)/O(v) \cong SO(w)/SO(v)$ if it is white. We saw the unitary groups $V_w(\mathbb{C}^w) \cong U(w)$ realized as GZ fibers in Example 3.5.13, so every complex and real Stiefel manifold except for the disconnected $V_w(\mathbb{R}^w) \cong O(w)$ occurs as a GZ fiber.

The direct product splitting in Corollary 3.5.1 is still not the end of the story on simplified descriptions of direct factors of GZ fibers. We make two further observations.

3.5.19 (Pinching). First, since $SO(1) = 1$, a “pinch” row of width 1 in a white component corresponds to a direct product splitting $X \otimes_{SO(1)} Y \cong X \times Y$, thus leading to a refinement of the direct product decomposition in Theorem 3.4.3 for an orthogonal Gelfand–Zeitlin fiber.

3.5.20 (Opportunistic splittings). Second, one can often split off Stiefel manifolds as direct factors. Indeed, if $M_1 \leq M_2$ in the notation of (3.5.8), then the map

$$\begin{aligned} U(M_1) \otimes_{U(m_1)} U(M_2) \otimes_{U(m_2)} Z &\longrightarrow \left(U(M_1)/U(m_1) \right) \times U(M_2) \otimes_{U(m_2)} Z, \\ g \otimes h \otimes z &\longmapsto (gU(m_1), gh \otimes z) \end{aligned}$$

is a diffeomorphism with inverse $(gU(m_1), h' \otimes z) \longmapsto g \otimes g^{-1}h' \otimes z$, and similarly if the groups are special orthogonal. One can repeat this until one encounters a local maximum width $M_p > M_{p+1}$. For factors corresponding to pattern components terminating before the top row, if $M_r < M_{r-1}$, one can also peel Stiefel factors from the right-hand side. The simplest examples for which this is not possible are

$$U(3) \otimes_{U(1)} U(2)/U(1) \quad \text{and} \quad U(3) \otimes_{U(1)} U(2) \otimes_{U(1)} U(3).$$

The direct factors of Corollary 3.5.1 can also be realized as biquotients, in a way clear from the proof of Proposition 3.4.13, Corollary 3.5.1, Proposition 3.5.6, and 3.5.7:

Proposition 3.5.21. *Every direct product factor of a GZ fiber can be written as a biquotient $A \backslash G/B$ as in Proposition 3.4.13.*

The following example applies our description to a more complicated unitary GZ fiber. To our knowledge, such examples have not been previously described in the literature.

Example 3.5.22. Consider the unitary GZ pattern in Figure 1.0.4. The double diamond on the left contributes $U(2) \otimes_{U(1)} U(2)$, or $S^3 \times U(2) \cong (S^3)^2 \times S^1$ by 3.5.20 and the decomposition $U(2) = \{\text{diag}(z, z^{-1}) : z \in U(1)\} \cdot SU(2)$. The long component on the right contributes $U(2)/U(1) \cong S^3$ as in Example 3.5.12. Finally, the largest component contributes $U(4) \otimes_{U(2)} U(3)/U(2)$. The factors associated to the remaining connected components are $U(1)$, as explained in Example 3.5.14. All told, the associated GZ fiber is diffeomorphic to

$$(S^1)^7 \times (S^3)^3 \times U(4) \otimes_{U(2)} U(3)/U(2),$$

where the last factor can equivalently be written as a biquotient $U(2) \backslash (U(4) \times U(3)) / U(2)$.

3.6. Circle factors

Some known observations concerning circle actions on and circle factors of Gelfand–Zeitlin fibers fall more or less immediately, and in more transparent form, out of our analysis.

3.6.1 (The determinant and circle extraction). The block-inclusions $U(d) \rightarrow U(d+1)$ (standard by Proposition 3.5.6) figuring in the iterated balanced products (3.5.8) and (3.5.9) evidently preserve determinants. Any unitary factor Y as in (3.5.8) corresponding to a component of the Gelfand–Zeitlin pattern not ending in the top row thus admits a well-defined determinant map to $U(1)$ given by **det**: $g_1 \otimes \cdots \otimes g_r \mapsto \det(g_1) \cdots \det(g_r)$. There is a natural right action of $U(1)$ on Y induced by the lower-right-corner block inclusion in $U(M_r)$, and thus

$$\begin{aligned} \det^{-1}(1) \times U(1) &\longrightarrow U(M_1) \otimes_{U(m_1)} \cdots \otimes_{U(m_{r-1})} U(M_r), \\ (g_1 \otimes \cdots \otimes g_r, z) &\longmapsto g_1 \otimes \cdots \otimes g_r \cdot z \end{aligned} \quad (3.6.2)$$

is a well-defined diffeomorphism, with inverse $x \mapsto (x \cdot (\det x)^{-1}, \det x)$. Thus every component of the Gelfand–Zeitlin pattern not ending in the top row contributes a circle factor to the fiber.

As for the other factor, $\det^{-1}(1)$, note that the natural map $\prod SU(M_j) \hookrightarrow \prod U(M_j) \twoheadrightarrow Y$ surjects onto it, as can be seen by iteratively replacing factors, using the left and right $U(1)$ -actions on each $U(m_j)$ induced by the lower-right-corner inclusion: $g_1 \otimes g_2 \otimes \cdots = g_1 \cdot (\det g_1)^{-1} \otimes (\det g_1) g_2 \otimes \cdots$ and so on. One can show a similar surjection if Y is of the form (3.5.9), corresponding to a factor ending in the top row, in which case the $U(1)$ -action on the right is quotiented out. Thus $\det^{-1}(1)$ equals

$$SU(M_1) \otimes_{SU(m_1)} \cdots \otimes_{SU(m_{r-1})} SU(M_r) \quad \text{or} \quad Y = SU(M_1) \otimes_{SU(m_1)} \cdots \otimes_{SU(m_{r-1})} SU(M_r) / SK_n. \quad (3.6.3)$$

These observations apply equally to the unitary factor F_U of an orthogonal GZ fiber. As noted in Example 3.5.15, width-2 white diamonds in a GZ pattern also contribute $SO(2)$ components to the corresponding fiber.

Notation 3.6.4. For a unitary Gelfand–Zeitlin system, let $t = t(p)$ be the number of components not ending in the top row of the Gelfand–Zeitlin pattern corresponding to p . (In other words, this is the number of Δ -shapes of width 1 in the first n rows.) For an orthogonal Gelfand–Zeitlin system, let $t(p)$ be the number of such components in the positive part of the GZ pattern, plus the number of diamonds of width 2 in the white components.

Considering all factors of $\Psi^{-1}(p)$ together, the product of the determinant maps is a map onto the torus $T^{t(p)}$ which we will call Det_p . Thus we have the following:

Proposition 3.6.5. *There is for each $p \in \Delta$ a $T^{t(p)}$ -equivariant diffeomorphism $T_p \cong \text{Det}_p^{-1}(1) \times T^{t(p)}$.*

In the unitary case, the splitting off of a T^t factor is result of Cho–Kim–Oh [CKO20, Thm. 6.11].

Corollary 3.6.6. *The fiber $\Psi^{-1}(p)$ over a point p in the interior of a unitary or orthogonal GZ polytope $\Delta_{\lambda(n+1)}$ is a torus.*

In the unitary case, this is result of Cho–Kim–Oh [CKO20, Thm. 6.14] and also of Bouloc–Miranda–Zung [BouMZ18, §5(b)].

3.6.7 (The topological Thimm trick and coordinates). We compare the torus action of 3.6.1 with the traditional torus action obtained by the Thimm trick (see Cho–Kim–Oh [CKO20] and Pabiniak [Pab12, §3.5]). In the notation from 2.1.6, each centralizer $Z_{H_j}(L_j)$ acts on $\Psi^{-1}(p)$ by $z_j \cdot \vartheta := g_j z_j g_j^{-1} \cdot \vartheta$, where the action on the left is the coadjoint action of G_{n+1} and the map $\varphi_n \circ \dots \circ \varphi_j$ has been suppressed. Putting these all together, we have an action of $\prod Z_{H_k}(L_k)$ on $\Psi^{-1}(p)$.¹⁵

Using 3.1.1 to convert from $\vartheta \in \Psi^{-1}(p)$ to $(g_k L_k) \in \Omega_p^r$, the entries of $z_j \cdot (g_k L_k)$ are given by

$$\begin{cases} g_k L_k, & k < j, \\ g_j z_j g_j^{-1} g_k L_k, & k \geq j, \end{cases}$$

where again $\varphi_{k-1} \dots \varphi_j$ is suppressed. The coordinate $k = j$ gives $(z_j \cdot (g_k L_k))_j = g_j z_j L_j$, but it is useful to absorb $k = j$ into the $k \geq j$ case to avoid case distinctions. Converting this action on Ω_p^r into an action on T_p using 3.4.4, one finds that only the j^{th} tensor-coordinate is changed under the action of $z_j \in Z_{H_j}(L_j)$, so that the point (3.4.6) maps to

$$a_\alpha g_\alpha \otimes a_{\alpha+1} g_\alpha^{-1} g_{\alpha+1} \otimes \dots \otimes a_{j-1} g_{j-2}^{-1} g_{j-1} \otimes a_j g_{j-1}^{-1} g_j z_j \otimes a_{j+1} g_j^{-1} g_{j+1} \otimes \dots \otimes a_n g_{n-1}^{-1} g_n L_n. \quad (3.6.8)$$

Factoring H_k and L_k respectively as $\bigoplus U(d_i)$ and $\bigoplus K_i$ as in (2.2.6) and (2.2.9), one evidently has $Z_{H_j}(L_j) = \bigoplus Z_{U(d_i)}(K_i)$, with $Z_{U(d_i)}(K_i) = Z(U(d_i))$ the diagonal copy of $U(1)$ if $U(d_i) = K_i$, and otherwise $Z_{U(d_i)}(K_i) \cong U(1) \times Z(K_i)$ if $K_i = [1] \oplus U(d_i - 1)$ (or $U(d_i - 1) \oplus [1]$), where the $U(1)$ factor corresponds to and acts on the r_i coordinate of $\zeta^{(j+1)}$ in (2.2.8). If we restrict our attention to factors $Z_{U(1)}(U(0))$, then on splitting T_p into direct factors of the form in (3.5.8), we see from (3.6.8) that the relevant $U(1)$ act only on the right of the final tensor-component of each direct factor, so this is the same action of $T^{t(p)}$ we introduced in 3.6.1.¹⁶

Theorem 3.6.9. *The torus action of 3.6.1 is that given by the Thimm trick.*

Remark 3.6.10. Bouloc–Miranda–Zung [BouMZ18, (5.9)] give a description of multi-diamond singularities of unitary GZ systems as a product of unitary groups (cf. Example 3.5.12), in particular observing that every direct factor corresponding to a diamond can be written as $U(n) \cong \text{SU}(n) \times U(1)$. This is of course a special case of Proposition 3.6.5.

¹⁵ It is clear from the definition that this action is continuous and does not depend on the chosen representative $g_j \in G_j/L_j$. To see the actions, for varying j , commute, note that $z_\ell \cdot g_j z_j g_j^{-1} \vartheta = \check{g}_\ell z_\ell \check{g}_\ell^{-1} (g_j z_j g_j^{-1} \vartheta)$ for \check{g}_ℓ^{-1} such that $\check{g}_\ell^{-1} (g_j z_j g_j^{-1} \vartheta^{(\ell)}) = \lambda^{(\ell)}$; if $\ell > j$, then $\check{g}_\ell^{-1} = g_\ell^{-1} (g_j z_j g_j^{-1})^{-1}$ works. On the other hand, $z_j \cdot g_\ell z_\ell g_\ell^{-1} \vartheta$ is just $g_j z_j g_j^{-1} g_\ell z_\ell g_\ell^{-1} \vartheta$ since $\Phi^{n+1-j}(g_\ell z_\ell g_\ell^{-1} \vartheta) = \vartheta^{(j)}$.

¹⁶ An interesting note is that the action of $Z_{H_j}(L_j)$ is typically noncanonical, as L_j depends on $\zeta^{(j+1)}$, which there are various reasonable choices of, but the action of T^t is uniquely defined.

Remark 3.6.11. Cho–Kim–Oh obtained Proposition 3.6.5 for a unitary GZ fiber, observing the other factor Y is a simply-connected manifold [CKO20, Theorem 6.11] (we will recover this more simply in Proposition 5.1.1). They obtain this decomposition in two steps, first observing the t GZ functions corresponding to the top vertices of each connected component in the GZ pattern with $k_t \leq n$ generate an action of T^t on the GZ fiber, and second using toric degenerations to show this T^t -action is free. Our recovery of this decomposition is more elementary, since we do not require a toric degeneration, and our decomposition is also finer, since Corollary 3.5.1 and (3.6.2) show the simply-connected space Y is the direct product of the spaces (3.6.3). On the other hand, their description has much more geometric content.

4. The local structure of a coadjoint orbit

We have just noted that Cho–Kim–Oh obtain the torus factor of Proposition 3.6.5, in the unitary case, as a consequence of a known toric degeneration, whose time-1 gradient-Hamiltonian flow induces a quotient map from \mathcal{O} to a certain toric variety X_0 . Our approach in Section 4.1 will allow us to go in the other direction, defining a map onto a toric manifold in both the unitary and the orthogonal cases without reference to geometry. Although the idea of this map is strikingly simple, in fact a triviality fiberwise, to show that the induced function on \mathcal{O} is continuous we will need to finally examine more than one GZ fiber at time, leading to local expressions over a face of the polytope in Section 4.2, and over the union of two faces in Section 4.3. These expressions in hand, we conclude the proof in Section 4.4.

4.1. Toric degeneration

We now attempt to relate the maps $\text{Det}_p: \Psi^{-1}(p) \rightarrow T^{t(p)}$ of Section 3.6 for varying p .

4.1.1. We will refer to the interior of any face of a Gelfand–Zeitlin polytope Δ as an *open face*¹⁷. As the Gelfand–Zeitlin pattern of any two points in the same open face E of the Gelfand–Zeitlin polytope $\Delta = \Delta_{\lambda^{(n+1)}}$ are the same, the function $t: \Delta \rightarrow \mathbb{Z}$ is constant on each open face. Since each open face is a convex subset of $\mathbb{R}^{\dim \Delta}$, hence contractible, and the fibers over each point of E are diffeomorphic, the restriction of Ψ to E is a trivial bundle, but we will provide an explicit diffeomorphism with the product bundle in Section 4.2.

Suppose now that $q \in \Delta$ lies in some codimension-one open face $F \subsetneq \overline{E}$. We will show in Section 4.3 that the inclusion $F \hookrightarrow \overline{E}$ induces a map $f: \Psi^{-1}(p) \rightarrow \Psi^{-1}(q)$ and a homomorphism $T^f: T^{t(p)} \rightarrow T^{t(q)}$ rendering commutative the square

$$\begin{array}{ccc} \Psi^{-1}(p) & \xrightarrow{\text{Det}_p} & T^{t(p)} \\ f \downarrow & & \downarrow T^f \\ \Psi^{-1}(q) & \xrightarrow{\text{Det}_q} & T^{t(q)}. \end{array} \quad (4.1.2)$$

These maps, taken altogether, express every $T^{t(p)}$ for $p \in \Delta$ as a quotient of $T = T^{\dim \Delta}$ in a well-defined and coherent way, so that $X_0 := \bigcup_{p \in \Delta} T^{t(p)}$ can naturally be identified with a

¹⁷ even though among these only the interior Δ° is actually an open subset of Δ

quotient of $T \times \Delta$, and hence inherits a T -action with orbit space $X_0/T = \Delta$. The T -space X_0 underlies a toric variety appropriately known as a *Gelfand–Zeitlin toric variety*. The various determinant maps compile into a surjective function $\text{Det}: \mathcal{O} \rightarrow X_0$ such that the composition with the projection $X_0 \rightarrow \Delta$ taking $T^{t(p)}$ to $\{p\}$ is the GZ system $\Psi: \mathcal{O} \rightarrow \Delta$, and we will show the following:

Theorem 4.1.3. *The map $\text{Det}: \mathcal{O}_{\lambda^{(n+1)}} \rightarrow X_0$ is well defined and continuous.*

This gives a sort of underlying topological model for a toric degeneration, simply the open mapping cylinder of the map $S^1 \times \mathcal{O} \rightarrow \mathcal{O} \xrightarrow{\text{Det}} X_0$, which fibers over the open disc in such a way that the generic fiber is \mathcal{O} and the special fiber is X_0 .

Remark 4.1.4. Nishinou–Nohara–Ueda [NNU10] construct flat toric degenerations $(X_t)_{t \in \mathbb{C}}$ with generic fiber $\mathcal{O}_{\lambda^{(n+1)}}$ and special fiber X_0 and prove using a limit argument that the Hamiltonian flow map ϕ from a subset of X_1 to X_0 continuously extends to be defined on all of X_1 . The construction of ϕ relies on solving a system of ODEs, and so is not easy to directly compare with what we have done here, but it is natural to expect that ϕ and Det agree up to a translation of each fiber $X_0|_p$ of X_0 by a continuously varying element of $T^{t(p)}$.

4.2. A local model over a face

To prove the claims leading to Theorem 4.1.3, we are forced to compare nearby factors.

4.2.1. Recall that the final pullback $F_\alpha^{n+1} = \Psi^{-1}(p)$ of Figure 2.1.3 could be given as the iterated fiber product (3.1.2), determined by the system of maps

$$\cdots \rightarrow G_k/H_k \leftarrow G_k/L_k \rightarrow G_{k+1}/H_{k+1} \leftarrow \cdots \rightarrow G_n/H_n \leftarrow G_n/L_n \rightarrow G_{n+1}/H_{n+1}, \quad (4.2.2)$$

where the leftward maps were projections and the rightward maps were described in Lemma 3.1.3. The groups H_k as described in 2.2.5 and 2.3.9 were the same for all $p \in E$ since we chose diagonal representatives $\lambda^{(k)}$. Similarly, by an appropriate choice of $\zeta^{(k+1)}$ in 2.2.7 and 2.3.11, we could take the L_k to all similarly be the same. Since the $\zeta^{(k)}$ are continuous functions in $p = (\lambda^{(n+1)}, \lambda^{(n)}, \dots, \lambda^{(1)})$, the $a_k = a_k(p)$ are as well. It follows that if we take the union of the zig-zags (4.2.2), where the objects are the same but we recall from 3.2.4 that the maps $G_k/L_k \rightarrow G_{k+1}/H_{k+1}$ depend on $p \in E$, then we obtain a system

$$\cdots \rightarrow E \times G_k/H_k \leftarrow E \times G_k/L_k \rightarrow E \times G_{k+1}/H_{k+1} \leftarrow \cdots \rightarrow E \times G_{n+1}/H_{n+1} \quad (4.2.3)$$

of continuous, fiber-preserving maps of product bundles over E , whose ultimate pullback Ω_E^r , restricted to any $p \in E$, is Ω_p^r . Then Ω_E^r is diffeomorphic to $\Psi^{-1}(E)$, since the evaluation map $(p, (g_k L_k)) \mapsto \varphi_n(g_n) \zeta_{n+1}(p)$ is smooth and bijective on fibers.

In Construction 3.2.1, we moved from Ω_p^r to Ω_p^c by replacing the original maps $G_k/L_k \rightarrow G_{k+1}/H_{k+1}$ by $g L_k \mapsto a_{k+1} \varphi_k(g) a_{k+1}^{-1} H_{k+1}$. Since each map $(p, g_{k+1} H_{k+1}) \mapsto (p, a_{k+1}(p) g_{k+1} H_{k+1})$ is a diffeomorphism, the diffeomorphism type of the pullback is unaffected if we insert these maps after the existing maps $E \times G_k/L_k \rightarrow E \times G_{k+1}/H_{k+1}$, and this shows the resulting final pullback Ω_E^c is diffeomorphic in a fiber-preserving fashion to Ω_E^r and hence to $\Psi^{-1}(E)$.

Then Theorem 3.4.3, applied fiberwise, yields a diffeomorphism from Ω_E^c to

$$T_E := (E \times H_\alpha) \otimes_{E \times L_\alpha} (E \times H_{\alpha+1}) \otimes_{E \times L_{\alpha+1}} \cdots \otimes_{E \times L_{n-1}} (E \times H_n)/(E \times L_n),$$

where the maps $E \times L_k \longrightarrow E \times H_k$ are inclusions and the maps $E \times L_k \longrightarrow E \times H_{k+1}$ are given by $(p, g) \longmapsto (p, a_{k+1}(p)\varphi_k(g)a_{k+1}(p)^{-1})$. As discussed in 3.4.4, although the elements $a_{k+1}(p) \in G_{k+1}$ continuously vary, the effect of the conjugation maps $L_k \longrightarrow H_{k+1}$ on unitary block components is the same for all $p \in E$. Hence there is a natural identification $T_E \cong E \times T_p$, and thus we also have an identification $\Psi^{-1}(E) \cong E \times T_p$.

4.2.4 (Coordinate (in)dependence). It follows from 4.2.1 that the expression given in (3.4.5) for the diffeomorphism $\Omega_E^c \xrightarrow{\sim} T_E$ does not depend on the point p either, despite the appearance of the $a_k(p)$ in the expression. From (3.4.6), however, we see the same cannot be said of the composite diffeomorphism $\Omega_E^r \xrightarrow{\sim} T_E$ where the expression does vary pointwise (nor, hence, can it be claimed of the total composite $\Psi^{-1}(E) \xrightarrow{\sim} \Omega_E^r \xrightarrow{\sim} \Omega_E^c \xrightarrow{\sim} T_E$) even though over each $p \in E$ it restricts to a diffeomorphism $\Omega_p^r \xrightarrow{\sim} T_p$.

4.3. A local model over two faces

Now we would like to understand $\Psi^{-1}(E \cup F)$ for \bar{F} a codimension-one face of \bar{E} . Intuitively speaking, since the fibers over E and over F are all the same, we expect that all we really need to understand is what happens over a ray from F into E . This turns out to be essentially correct.

4.3.1. Select a point $p \in F$ and suppose that μ is the eigenvalue labelling the component merged from two components in the pattern of E . We will consider the intersection with \bar{E} of the affine 2-plane P in which the $\lambda_j^{(k)}$ corresponding to all components except those merging to the μ -component of F are fixed. Let λ^+ and λ^- denote the greatest and least of these and μ^+ and μ^- the labels on the merging components. Then we are focusing attention on the region $\lambda^+ > \mu^+ \geq \mu^- > \lambda^-$ of P and interested in what happens as $|\mu^\pm|$ approach one another or 0. The numbers $\mu = \frac{1}{2}(\mu^+ + \mu^-)$ and $t = \frac{1}{2}(\mu^+ - \mu^-)$ also serve as coordinates on this region, and we for now fix μ as well and consider what happens as $t \rightarrow 0$, which is to say $\mu^\pm \rightarrow \mu$. So we consider a closed interval $\gamma \subsetneq P$ as parameterized by $t \in [0, \varepsilon_\mu]$.

4.3.2 (The effect on passing to a codimension-one face on H_k). The block-diagonal group H_k which is $H_k(q) = \text{Stab}_{\text{U}(k)} \lambda^{(k)}(q)$ for $p \neq q \in \gamma$ is a subgroup of $\bar{H}_k = \text{Stab}_{\text{U}(k)} \lambda^{(k)}(p)$. For those rows in which the GZ patterns of E and F agree, we have $H_k = \bar{H}_k$. On the other hand, in a row where they disagree, we have a case distinction.

- First assume that the corresponding block factors are standard unitary (which is always the case for a unitary GZ fiber). If μ^+ occurs m^+ times and μ^- m^- times in $\lambda^{(k)}(q)$, then μ occurs $m^+ + m^-$ times in $\lambda^{(k)}(p)$, and the inclusion $H_k \hookrightarrow \bar{H}_k$ is the identity on the blocks corresponding to eigenvalues other than μ^+ , μ , and μ^- , and on these blocks, it is $\text{U}(m^+) \oplus \text{U}(m^-) \hookrightarrow \text{U}(m^+ + m^-)$.

For an orthogonal GZ fiber, consulting (2.3.2), (2.3.5), and (2.3.4), there are several more possibilities for the nontrivial blocks of the inclusion $H_k \hookrightarrow \bar{H}_k$.

- If k is even with $U_\ell < H_k$ nonstandard with label μ^- and $\text{U}(d_{\ell-1})$ standard with label μ^+ , the block map is $\text{U}(d_{\ell-1}) \oplus \text{U}(d_\ell)^o \hookrightarrow \text{U}(d_{\ell-1} + d_\ell)^{\text{id} \oplus o}$.
- If k is even, $U_\ell = \text{U}(1) < H_k$ corresponds to $\mu^- < 0$, and $\mu^+ > -\mu^-$ corresponds to $\text{U}(d_{\ell-1})$, then as $|\mu^+| - |\mu^-| \rightarrow 0$, the block map is $\text{U}(d_{\ell-1}) \oplus \text{U}(1) \hookrightarrow \text{U}(d_{\ell-1} + 1)^o$.

- If $-\mu^- = 0$ and U_ℓ corresponds to μ^+ , the block map is $U_\ell \oplus \text{SO}(d_0) \hookrightarrow \text{SO}(2d_\ell + d_0)$.

4.3.3 (The effect on passing to a codimension-one face on L_k). The possibilities for the shapes of the merging (μ^+ - and μ^- -labelled) components in rows k and $k+1$ are precisely the following:

$$\square\square, \quad \triangle\square, \quad \square\square, \quad \square\square, \quad \square\square, \quad \square\square, \quad \square\square, \quad \square\square.^{18}$$

In six of the cases, we have $L_k(q) = L_k \leq \bar{L}_k = L_k(p)$ for our usual choices of orbit representatives $\zeta^{(k+1)}(q)$. In the cases $\square\square$ and $\square\square$, the usual representatives do not make this true, but in these cases one can select a different smooth family of representatives $\zeta^{(k+1)}(q)$ per the caution in 2.2.7 such that again $L_k \leq \bar{L}_k$. (We suppress the details of this analysis.) These groups are then connected by the commutative diagram

$$\begin{array}{cccccccc} \cdots & \longrightarrow & H_k & \longleftarrow & L_k & \longrightarrow & H_{k+1} & \longleftarrow & L_{k+1} & \longrightarrow & \cdots \\ & & \downarrow & & \downarrow & & \downarrow & & \downarrow & & \\ \cdots & \longrightarrow & \bar{H}_k & \longleftarrow & \bar{L}_k & \longrightarrow & \bar{H}_{k+1} & \longleftarrow & \bar{L}_{k+1} & \longrightarrow & \cdots, \end{array}$$

inducing a smooth map

$$T_q = H_\alpha \otimes_{L_\alpha} H_{\alpha+1} \otimes_{L_{\alpha+1}} \cdots \otimes_{L_{n-1}} H_n/L_n \longrightarrow \bar{H}_\alpha \otimes_{\bar{L}_\alpha} \bar{H}_{\alpha+1} \otimes_{\bar{L}_{\alpha+1}} \cdots \otimes_{\bar{L}_{n-1}} \bar{H}_n/\bar{L}_n = T_p \quad (4.3.4)$$

for $q \in \gamma \setminus \{p\}$. Our goal is to identify $\Psi^{-1}(\gamma)$ with the mapping cylinder¹⁹ of this map.

Let us agree to write $\gamma \cdot G_k/H_k$ for the mapping cylinder of the quotient map $G_k/H_k \longrightarrow G_k/\bar{H}_k$ and similarly write $\gamma \cdot G_k/L_k$. Then the continuity of $a_k(q)$ gives us a continuous map $\gamma \cdot G_k/L_k \longrightarrow \gamma \cdot G_{k+1}/L_{k+1}$ taking $[q, gL_k(q)] \mapsto [q, \varphi_k(g)a_{k+1}(q)^{-1}H_k(q)]$, and putting these together, we obtain a “ γ -variant” of (4.2.3). We claim that the final pullback Ω_γ^r of the staircase ending in this zig-zag is indeed homeomorphic to $\Psi^{-1}(\gamma)$. Indeed, Ω_γ^r is equipped with a natural map to γ and for each $q \in \gamma$ there is a diffeomorphism $\omega_q: \Omega_\gamma^r \longrightarrow \Psi^{-1}(q)$. As an iterated fiber product, Ω_γ^r comprises those lists $((g_k L_k(q)) \in \prod_{k=1}^n G_k/L_k(q)$ satisfying the equations $\varphi_k(g_k)a_{k+1}^{-1}H_{k+1} = g_{k+1}H_{k+1}$ for $1 \leq k \leq n-1$; under this identification, ω_q is given by $(g_k L_k(q)) \mapsto \text{Ad}_{\varphi_n(g_n)}^* \zeta^{(n)}(q)$. As $q \mapsto \zeta^{(n)}(q)$ is continuous, it follows $\omega: [q, (g_k L_k(q))] \mapsto \omega_q(g_k L_k(q))$ is a continuous bijection $\Omega_\gamma^r \longrightarrow \Psi^{-1}(\gamma)$. Since Ω_γ^r is compact and $\Psi^{-1}(\gamma)$ Hausdorff, ω is a homeomorphism.

As expected, replacing the maps $\gamma \cdot G_k/L_k \longrightarrow \gamma \cdot G_{k+1}/H_{k+1}$ with

$$[q, gL_k(q)] \mapsto [q, a_{k+1}(q)\varphi_k(g)a_{k+1}(q)^{-1}H_k(q)]$$

yields a space Ω_γ^c homeomorphic to Ω_γ^r . To state the appropriate variant of Theorem 3.4.3, let $\gamma \cdot H_k$ denote the mapping cylinder $[0, \varepsilon_\mu] \times H_k \cup \{0\} \times \bar{H}_k$ of $H_k \hookrightarrow \bar{H}_k$, and similarly for $\gamma \cdot L_k$. Then as expected, we find a homeomorphism of Ω_γ^c with

$$T_\gamma := \gamma \cdot H_\alpha \otimes_{\gamma \cdot L_\alpha} \gamma \cdot H_{\alpha+1} \otimes_{\gamma \cdot L_{\alpha+1}} \cdots \otimes_{\gamma \cdot L_{n-1}} \gamma \cdot H_n/\gamma \cdot L_n.^{20}$$

¹⁸ There are two possible answers each to three independent questions: (1) Is the slant separating the two shapes left- or right-facing? (2) (resp., (3)) Is the left (resp., right) shape a parallelogram or a trapezoid?

¹⁹ Recall that the *mapping cylinder* of a continuous map $f: X \longrightarrow Y$ of topological spaces is the quotient of the disjoint union of $X \times [0, 1]$ and Y by the equivalence relation setting $(x, 1) \sim f(x)$.

²⁰ One can then transfer over the smooth structure if one wishes.

As we observed in 3.4.4, for the maps $L_k \rightarrow H_{k+1}$ determining T_p for $p \in F$ do not depend on p , so the T_q are all the same for $t > 0$ and T_γ is itself a mapping cylinder, that of the map (4.3.4). Now we note that this whole discussion fixed, but did not depend upon the particular value of μ , but groups H_k, \bar{H}_k, L_k , and \bar{L}_k depended only whether or not t was 0, and again, the maps between them, induced by the $a_k(q)$, do not depend on μ which are continuous in q within the region we are considering. We may select a closed rectangular neighborhood $R_P = [\mu_0, \mu_1] \times [0, \varepsilon_P]$ of p within P in μt -coordinates, where ε_P is the minimum value $\varepsilon_{\mu'}$ for $\mu' \in [\mu_0, \mu_1]$. Then varying μ in the above argument and replacing each e_μ with ε_P , we have homeomorphisms of $\Psi^{-1}(R_P)$ with what we may call $\Omega_{R_P}^r, \Omega_{R_P}^c$, and T_{R_P} . Again by the fact observed in 3.4.4 that the maps $L_k \rightarrow H_{k+1}$ do not depend on $q \in E$ and $\bar{L}_k \rightarrow \bar{H}_{k+1}$ do not depend on $p \in F$, we see T_{R_P} is homeomorphic to $[\mu_0, \mu_1] \times T_\gamma$. (To be sure, as in 3.4.4, the expressions for the maps $\Omega_\gamma^r \rightarrow T_\gamma$ do indeed depend on μ , even though $\Omega_\gamma^c, T_\gamma$, and the homeomorphism $\Omega_\gamma^c \rightarrow T_\gamma$ do not.)

Now we may equally well vary P and hence R_P by moving the $\lambda_j^{(k)}$ labeling the non-merging components of the GZ pattern over E and F in such a way as to not collide. By the independence of T_p and T_q from these choices we have just observed, we finally find the following.

Theorem 4.3.5. *For U a small enough neighborhood of $p \in \bar{E}$, we have homeomorphisms*

$$\Psi^{-1}(U) \xrightarrow{\cong} \Omega_U^r \xrightarrow{\cong} \Omega_U^c \xrightarrow{\cong} T_U \xrightarrow{\cong} (U \cap F) \times T_\gamma,$$

where T_γ is the mapping cylinder of the map (4.3.4).

4.4. Consistency and continuity of the determinant

Now we can show the map Det of Section 4.1 is well-defined and consistent.

Proof of Theorem 4.1.3. By 4.2.1, over an open face E of Δ , we may define a determinant map by

$$\Psi^{-1}(E) \xrightarrow{\sim} E \times T_q \longrightarrow T_q \xrightarrow{\text{Det}} T^{t(q)},$$

where we have seen the particular point $q \in E$ chosen does not affect the map, and by 4.3.1, for F the interior of a face $\bar{F} \subsetneq \bar{E}$ and $U \subseteq \bar{E}$ a sufficiently small neighborhood of $p \in F$, we have $\Psi^{-1}(U) \approx (U \cap F) \times T_\gamma$, where T_γ is the mapping cylinder of the map f of (4.3.4). Fixing μ with $\{p\} = \gamma \cap F$ and a $q \in \gamma \cap E$, we claim there is a commutative square as in (4.1.2), inducing a map of mapping cylinders from T_γ to the mapping cylinder $X_0|_\gamma$ of T^f . Granted this, composing through

$$\Psi^{-1}(U) \longrightarrow (U \cap F) \times T_\gamma \twoheadrightarrow T_\gamma \longrightarrow X_0|_U$$

gives a continuous, well-defined map Det_U agreeing with the previously defined Det_p for $p \in F$ and Det_q for $q \in E$. As $p \in F$ was arbitrary, this defines Det continuously on $\Psi^{-1}(E \cup F)$.

To see the commutativity of (4.1.2), we note two combinatorial possibilities. First, if the GZ pattern associated to F arises from that of E by joining two components not meeting the top row, then $L_n = \bar{L}_n$, but the maps $U(m^+) \oplus U(m^-) \rightarrow U(m^+ + m^-)$ on the components of H_k corresponding to merging components induce $\deg(g) \oplus \deg(h) \mapsto \det(g \oplus h) = \det(g) \det(h)$. Thus in this case the map $T^f: T^{t(p)} \rightarrow T^{t(q)}$ is of the form $\text{id} \times \mu \times \text{id}$ where μ multiplies the i^{th} and $(i+1)^{\text{st}}$ $U(1)$ coordinates. Second, if in the pattern for F , the i^{th} component of the pattern of E becomes joined with the top row, the map $H_n/L_n \rightarrow \bar{H}_n/\bar{L}_n$ restricted to the relevant components is of the form $U(m^+) \oplus U(m^-)/U(m') \rightarrow U(m^+ + m^-)/U(m')$ (or symmetrically

swapping $+$ and $-$). The effect on determinants is that the coordinate coming from the i^{th} factor, labeled in the pattern by λ^+ and corresponding to $U(m^+)$ in the domain of this map, drops out, so in this case $T^f: T^{t(p)} \rightarrow T^{t(q)}$ projects out the i^{th} coordinate. Either way, the square commutes.

We now inductively extend the definition over all of Δ . To begin, for a vertex $p \in \Delta$, we have Det_p defined on $\Psi^{-1}(p)$ already by Proposition 3.6.5. Suppose we have already proven Det is defined and continuous on the union $\mathcal{O}^{\leq m} \subseteq \mathcal{O}$ of Ψ -preimages of faces of Δ of dimension $\leq m$, in such a way that the definition over each open face is that of Section 4.2. Each dimension- $(m+1)$ face \bar{E} is bounded by dimension- m faces; let \bar{F} be one of them. We can then use the first paragraph to define Det continuously on $\Psi^{-1}(E \cup F)$. We can equally well do this on $\Psi^{-1}(E \cup F')$ for any other face \bar{F}' of \bar{E} . If all these extensions over E agree, then we will have extended Det in a well-defined and continuous manner to $\mathcal{O}^{\leq m} \cup \Psi^{-1}(E)$, and we can do this independently for each E of dimension $m+1$ to complete the induction.

To see the extensions agree, note that the process of Section 4.3 depends on a choice of representatives $\zeta^{(k+1)}$,²¹ but that by Remark 2.2.11 and 2.3.11, these choices are related by $'\zeta^{(k+1)} = \varphi_k(h)\zeta^{(k+1)}$ for an $h = \bigoplus u_i \in \bigoplus_{i=1}^{\ell} \text{SU}(d_i) \oplus \text{SO}(d_0)$. We have seen in 3.1.7 and (3.4.6) that this coordinate change takes the tensor-coordinate $a_k g_{k-1}^{-1} g_k$ to $a_k g_{k-1}^{-1} g_k h^{-1}$ and does not affect the other coordinates. This means Det as computed with respect to $'\zeta^{(k+1)}$ and $\zeta^{(k+1)}$ is the same: only the circle component of Det corresponding to the pattern component containing the Δ -shape is affected by the transition, and this component of Det is multiplied by $\det(u_i) = 1$. \square

5. Algebro-topological invariants

In this section we apply the results of Section 3 to homotopy groups and cohomology rings.

5.1. Homotopy groups

From the balanced product presentation of Theorem 3.4.3 and the factorization of Corollary 3.5.1 into terms of the form (3.5.8) and (3.5.9), we can easily recover the first three homotopy groups of a Gelfand–Zeitlin fiber.

Proposition 5.1.1 (Cho–Kim–Oh [CKO20, Prop. 6.13]). *The fundamental group $\pi_1(\Psi^{-1}(p))$ of a unitary Gelfand–Zeitlin fiber is free abelian of rank $t(p)$, the number of components of the Gelfand–Zeitlin pattern not ending in the top row, whereas $\pi_2(\Psi^{-1}(p))$ is trivial.*

Proof. By Proposition 3.6.5, $\Psi^{-1}(p)$ is the direct product of a torus $T^{t(p)}$ and a factor $\text{Det}_p^{-1}(1)$, which by Corollary 3.5.1 is a direct product of factors Y_i of the form (3.6.3). The result follows from the long exact homotopy sequences of $\prod \text{SU}(m_j) \rightarrow \prod \text{SU}(M_j) \rightarrow Y_i$. \square

The same sequence recovers $\pi_3(Y_i)$ as the cokernel of $\pi_3(\prod \text{SU}(m_j) \rightarrow \prod \text{SU}(M_j))$. Since $\text{SU}(m) \hookrightarrow \text{SU}(n)$ induces an isomorphism on $\pi_3 \cong \mathbb{Z}$ for $n \geq m \geq 2$, one finds the following.

Proposition 5.1.2. *The third homotopy group $\pi_3(\Psi^{-1}(p))$ of a unitary Gelfand–Zeitlin fiber is free abelian. Its rank is the number of components of the graph obtained from the Gelfand–Zeitlin pattern by deleting rows of width 1 from each component, then deleting any components still meeting the top row.*

²¹ Indeed, in the situation $\nabla \Delta \nabla$, specializing to $\square \nabla$ by letting the eigenvalues of $\nabla \Delta$ approach one another and to $\nabla \square$ by letting the eigenvalues of $\Delta \nabla$ approach one another require different choices of $\zeta^{(k+1)}$.

Similar reasoning also applies in the case of an orthogonal Gelfand–Zeitlin fiber $\Psi^{-1}(p)$. Recall from Notation 3.5.2 that $\Psi^{-1}(p)$ is the direct product of a unitary part F_U that behaves like a unitary Gelfand–Zeitlin fiber and another factor F_{SO} .

Proposition 5.1.3. *The factor F_{SO} splits as a direct product of a torus $T \cong \mathrm{SO}(2)^t$ and a space Y with $\pi_1(Y) \cong (\mathbb{Z}/2)^s$ and $\pi_2(Y) \cong \mathbb{Z}^f$ and $\pi_3(Y) \cong \mathbb{Z}^g$, where t , s , and f are determined from the white components of the associated Gelfand–Zeitlin pattern: t is the number of local maxima of width 2, f is the number of local minima of width 2, possibly including the top row, and s is determined by counting the remaining white components remaining after the union of all diamonds of width 2 is deleted, then any resulting component containing 2 or more vertices in the top row is also deleted. We determine g as a sum of numbers h given in terms of the description of factors Y_i as in (3.5.8) and (3.5.9): if N_4 is the number of j such that $M_j = 4$, while $n_{\geq 3}$ is the number with $m_j \geq 3$, then $h = r + N_4 - n_{\geq 3}$.*

Proof. We noted in Example 3.5.12 that each diamond of width 2 contributes an $\mathrm{SO}(2)$ factor. It is then an exercise to examine each Y_i separately using the long exact homotopy sequence of the bundle $\prod \mathrm{SO}(m_j) \rightarrow \prod \mathrm{SO}(M_j) \rightarrow Y_i$. The key facts are that π_2 of a Lie group is trivial, π_3 of a simple Lie group is \mathbb{Z} , and the subgroup inclusions $\mathrm{SO}(m) \hookrightarrow \mathrm{SO}(n)$ induce an isomorphism on $\pi_1 \cong \mathbb{Z}/2$ for $m \geq 3$ and the surjection $\mathbb{Z} \twoheadrightarrow \mathbb{Z}/2$ for $m = 2$. \square

5.2. Cohomology of unitary Gelfand–Zeitlin fibers

In this section we compute the cohomology of the fibers of Gelfand–Zeitlin systems on unitary coadjoint orbits. Our result is summarized in the following theorem.

Theorem 5.2.1. *The integer cohomology ring of a unitary GZ fiber is isomorphic to the exterior algebra*

$$\Lambda[z_{2d-1,i}], \quad |z_{2d-1,i}| = 2d - 1.$$

where the generators $z_{2d-1,i}$ enumerate all Δ -shapes in the associated Gelfand–Zeitlin pattern with width d , i.e., d vertices on the long edge.

We demonstrate this result with an example before proceeding to the proof.

Example 5.2.2. Enumerating Δ -shapes in the GZ pattern in Figure 1.0.4, we see that the integral cohomology ring of the associated GZ fiber is

$$\Lambda[z_{1,1}, z_{1,2}, z_{1,3}, z_{1,4}, z_{1,5}, z_{1,6}, z_{1,7}, z_{3,1}, z_{3,2}, z_{3,3}, z_{5,1}, z_{5,2}, z_{7,1}], \quad |z_{m,j}| = m.$$

Note that isolated vertices in the top row of the GZ pattern do not count as Δ -shapes of width 1.

We now use the Serre exact sequence to compute the cohomology of the space $F_1^{n+1} \cong \Psi^{-1}(p)$ in Figure 2.1.3. We will write $G_k = \mathrm{U}(k)$ and $F^k := F_1^k$, and ι for the embedding $G_k/L_k \hookrightarrow G_{k+1}/H_{k+1}$ of Lemma 3.1.3. All cohomology will be taken with \mathbb{Z} coefficients.

Lemma 5.2.3. *The Serre spectral sequence of each bundle $F^{k+1} \rightarrow F^k$ collapses at E_2 .*

Proof. Let $\chi_k: \mathrm{U}(k)/H_k \rightarrow BH_k$ be a classifying map for the principal H_k -bundle $\mathrm{U}(k) \rightarrow \mathrm{U}(k)/H_k$, and write $j_k: F^k \rightarrow F_k^k = \mathrm{U}(k)/H_k$ for the composition of horizontal in Figure 2.1.3. We prove by induction on k that $\chi_k \circ j_k$ induces the zero map in reduced cohomology. This is so for $k = 1$ because F^1 is a point. For the induction step, factor j_{k+1} as the composite of $\tilde{j}_k: F^{k+1} \rightarrow F_k^{k+1} =$

$U(k)/L_k$ and ι and let $\tilde{\chi}_k: U(k)/L_k \rightarrow BL_k$ be a classifying map for the principal L_k -bundle $U(k) \rightarrow U(k)/L_k$. If we model BL_k as EH_k/L_k , then we have a map of H_k/L_k -bundles, shown in the bottom two rows of (5.2.4).

$$\begin{array}{ccccc}
 & & G_{k+1}/H_{k+1} & \xrightarrow{\chi_{k+1}} & BH_{k+1} \\
 & \nearrow^{j_{k+1}} & \uparrow \iota & & \uparrow \\
 F^{k+1} & \xrightarrow{\tilde{j}_k} & G_k/L_k & \xrightarrow{\tilde{\chi}_k} & BL_k \\
 \downarrow & & \downarrow & & \downarrow \\
 F^k & \xrightarrow{j_k} & G_k/H_k & \xrightarrow{\chi_k} & BH_k
 \end{array} \tag{5.2.4}$$

Consider the induced diagram in reduced cohomology. Since each $H^*BU(m+1) \rightarrow H^*BU(m)$ is a surjection, so is $H^*(BH_k) \rightarrow H^*(BL_k)$. By the inductive assumption, the bottom map $j_k^* \circ \chi_k^*$ is trivial, so it follows $\tilde{j}_k^* \circ \tilde{\chi}_k^*$ is trivial and hence so is $j_{k+1}^* \circ \chi_{k+1}^*$, concluding the induction.

For the collapse, note that every exterior generator z of the ring $H^*(H_k/L_k)$ transgresses in the spectral sequence of $BL_k \rightarrow BH_k$ to some τz , as one sees comparing the spectral sequences of the factors $BU(m) \xrightarrow{\cong} BU(m)$ and $BU(m) \rightarrow BU(m+1)$. But the map of H_k/L_k -bundles on the bottom in (5.2.4) induces a map of Serre spectral sequences, so z transgresses to $(\chi_k \circ j_k)^* \tau z = 0$ in the spectral sequence of $F^{k+1} \rightarrow F^k$. \square

Proof of Theorem 5.2.1. We show by induction on k that $H^*(F^k) \cong \bigotimes_{\ell=1}^{k-1} H^*(H_\ell/L_\ell)$ as graded rings, where H_k/L_k were identified in 2.2.7. For $k=1$, this is because the product is empty and F^1 is a point. For the induction step, the Serre spectral sequence of $F^{k+1} \rightarrow F^k$ collapses at E_2 by Lemma 5.2.3, so that associated graded algebra of $H^*(F^{k+1})$ is $H^*(F^k) \otimes H^*(H_k/L_k)$. This is a free abelian group by the inductive hypothesis, so there is no additive extension problem and in particular no 2-torsion. The lifts of a set of exterior generators for $H^*(H_k/L_k)$ along the fiber restriction $H^*(F^{k+1}) \rightarrow H^*(H_k/L_k)$ thus square to zero and hence generate an exterior subalgebra $\Lambda \cong H^*(H_k/L_k)$ within $H^*(F^{k+1})$. A basis of Λ also forms a basis for $H^*(F^{k+1})$ as an $H^*(F^k)$ -module, by the collapse and absence of an additive extension problem, so $H^*(F^{k+1})$ is the tensor product of Λ and $H^*(F^k)$, concluding the induction. \square

Knowing the cohomological structure also makes available a very natural homological description. Recall that the Künneth theorem and the multiplication of a topological group G , induce a graded ring structure on $H_*(G; k)$ for any choice of coefficient ring k , called the *Pontrjagin ring*, and a homomorphism $H \rightarrow G$ makes $H_*(G; k)$ a module over $H_*(H; k)$. This particularly holds for an inclusion $U(m) \rightarrow U(M)$ and the quotient map $U(m) \rightarrow *$. Using Theorem 5.2.1 and counting ranks, one finds the following.

Proposition 5.2.5. *Let a space X be given as on the left in (3.5.8) or (3.5.9) be given, writing $U(q)$ for the trivial group $U(0) = 1$ in the former case and for K_n in the latter. Then the projection of the fiber bundle*

$$\prod_{p=1}^{r-1} U(m_p) \times U(q) \rightarrow \prod_{p=1}^r U(M_p) \rightarrow U(M_1) \otimes_{U(m_1)} \cdots \otimes_{U(m_{r-1})} U(M_r)/U(q) = X$$

induces a surjection in homology and an identification

$$H_*(X) \cong H_*U(M_1) \otimes_{H_*U(m_1)} \cdots \otimes_{H_*U(m_{r-1})} H_*U(M_r) \otimes_{H_*U(q)} \mathbb{Z}.$$

This is similar to the reasoning that allowed us to compute π_3 in Proposition 5.1.2.

5.3. Cohomology of orthogonal Gelfand–Zeitlin fibers

The computation of the cohomology of a Gelfand–Zeitlin fiber is more interesting in the orthogonal case.

Notation 5.3.1. We extend the diagram of Figure 2.1.3 for an orthogonal Gelfand–Zeitlin fiber to $\alpha = 1$ by taking $G_k = H_k = L_k = \text{SO}(1)$ and setting $F^k = F_1^k$. We write $F = F^{n+1}$ for the Gelfand–Zeitlin fiber itself. We decomposing H_k and L_k respectively as $H_k^{\text{U}} \times H_k^{\text{SO}}$ and $L_k^{\text{U}} \times L_k^{\text{SO}}$ with H_k^{U} and L_k^{U} products of unitary groups and H_k^{SO} and L_k^{SO} orthogonal.

Both F_{U} and F_{SO} themselves admit tower descriptions as in Figure 2.1.3, given by taking F_k^k and F_k^{k+1} to respectively be $\text{SO}(k)/H_k^{\text{U}}$ and $\text{SO}(k)/L_k^{\text{U}}$ in the former case and $\text{SO}(k)/H_k^{\text{SO}}$ and $\text{SO}(k)/L_k^{\text{SO}}$ in the latter. Because the quotients $H_k^{\text{U}}/L_k^{\text{U}}$ are products of odd-dimensional spheres, Theorem 5.2.1 and Propositions 3.6.5, 5.2.5, and 5.1.2 and their proofs apply to give the following.

Proposition 5.3.2. *Given an orthogonal Gelfand–Zeitlin fiber F , the factor F_{U} is itself the product of a torus T and a space Y with $\pi_1(Y) = 0 = \pi_2(Y)$. The dimension of T is the number of Δ -shapes of width 1 in the positive part of the Gelfand–Zeitlin pattern.*

Theorem 5.3.3. *Given an orthogonal Gelfand–Zeitlin fiber F , the cohomology ring $H^*(F_{\text{U}}; \mathbb{Z})$ is an exterior algebra $\Lambda[z_{2d-1,i}]$, where the generators $z_{2d-1,i}$ of degree $2d - 1$ are enumerated by black Δ -shapes of width d in the positive part of the Gelfand–Zeitlin pattern.*

Since $H^*(F_{\text{U}})$ is free abelian, the Künneth theorem shows $H^*(F)$ is isomorphic as a graded ring to $H(F_{\text{U}}) \otimes H^*(F_{\text{SO}})$, so we focus exclusively on F_{SO} for the rest of the section.

We have seen in 3.5.10 that every Stiefel manifold is realized as a GZ fiber and in 3.5.10 that F_{SO} is the total space of tower of bundles of real Stiefel manifolds $V_p = \text{SO}(M_p)/\text{SO}(m_p)$,

$$\begin{array}{ccccccc}
 V_r & & V_{r-1} & & V_{r-2} & & \cdots & & V_3 & & V_2 \\
 \downarrow i_r & & \downarrow i_{r-1} & & \downarrow i_{r-2} & & & & \downarrow i_3 & & \downarrow i_2 \\
 F_{\text{SO}} & \longrightarrow & F^{\ell_{r-1}} & \longrightarrow & F^{\ell_{r-2}} & \longrightarrow & \cdots & \longrightarrow & F^{\ell_3} & \longrightarrow & F^{\ell_2} & \longrightarrow & V_1,
 \end{array} \tag{5.3.4}$$

which will play the same role for $H^*(F_{\text{SO}})$ that Figure 2.1.3 did for the unitary Theorem 5.2.1.

Lemma 5.3.5. *In the tower (5.3.4), the integral cohomology Serre spectral sequence of each bundle $V_p \rightarrow F^{\ell_p} \rightarrow F^{\ell_{p-1}}$ collapses.*

Thus most of what we have to say about the cohomology of F_{SO} is a consequence of facts about the cohomology of a Stiefel manifold, which we now discuss.

Examples 5.3.6. Following Examples 3.5.13 and 3.5.18, we see any $\text{SO}(M)$ and more generally any $V_{M-m}(\mathbb{R}^M) = \text{SO}(M)/\text{SO}(m)$ arises as a Gelfand–Zeitlin fiber, so a general description of the ring $H^*(F_{\text{SO}})$ is at least as hard as that of $H^*V_k(\mathbb{R}^m)$. The simplest non-sphere Stiefel manifolds, $V_2(\mathbb{R}^m)$ already give an example of the failure of the analogue of Lemma 5.2.3 in the orthogonal case. Indeed, the Serre spectral sequence of the associated sphere bundle $\frac{\text{SO}(m-1)}{\text{SO}(m-2)} \rightarrow \frac{\text{SO}(m)}{\text{SO}(m-2)} \rightarrow \frac{\text{SO}(m)}{\text{SO}(m-1)}$ supports a differential taking $z = 1 \otimes [S^{m-2}]$ to $\chi(S^{m-1})$ times $s = [S^{m-1}] \otimes 1$, which is nonzero when m is odd. It follows that the cohomology ring is $H^*(V_2(\mathbb{R}^m)) \cong \Lambda[z, s]$ when m is even, for any coefficients, whereas when $m = 2k + 1$ is odd, the cohomology rings over $\mathbb{Z}[1/2]$ and \mathbb{Z} are respectively $\Lambda[zs]$ and $\mathbb{Z}[s] \otimes \Lambda[z]/(2s, s^2, sz)$.

For another relatively simple example, the cohomology rings of $\text{SO}(4)$ over $\mathbb{Z}[1/2]$ and \mathbb{Z} are respectively $\Lambda[z, q]$ and $\mathbb{Z}[s] \otimes \Lambda[z, q]/(2y, y^2, sq)$, where $|y| = 2$ and $|z| = |q| = 3$.

Čadek, Mimura, and Vanžura [ČaMV03] have found a presentation of $H^*V_k(\mathbb{R}^M)$ which we will summarize some only some aspects of Proposition 5.3.9, as it is rather complicated.²²

Notation 5.3.7. In the Bockstein long exact sequence of cohomology groups of a space X arising from the short exact sequence $0 \rightarrow \mathbb{Z} \rightarrow \mathbb{Z} \rightarrow \mathbb{Z}/2 \rightarrow 0$ of coefficient rings, we write $\beta: H^{*-1}(X; \mathbb{F}_2) \rightarrow H^*(X)$ for the connecting map and $\rho: H^*(X) \rightarrow H^*(X; \mathbb{F}_2)$ for the reduction map, which is a ring homomorphism. The first Steenrod square is $\text{Sq}^1 = \rho\beta: H^{*-1}(X; \mathbb{F}_2) \rightarrow H^*(X; \mathbb{F}_2)$. We also write $\overline{H}^*(X) = H^*(X)/\text{torsion}$.

Definition 5.3.8. Let k be \mathbb{Z} or a finite quotient thereof, A a commutative graded algebra, and M a submodule of A free over k . We say M *admits a simple system of generators* if there are elements $v_j \in M$ such that the distinct monomials $v_{j_1} \cdots v_{j_\ell}$ of degree 0 or 1 in each v_j form a k -basis of M .²³

Proposition 5.3.9 (Čadek–Mimura–Vanžura [ČaMV03]). *The cohomology ring $H^*(\text{SO}(M)/\text{SO}(m); \mathbb{F}_2)$ admits a system of one simple generator v_i of each degree $i \in [m, M-1]$ with $v_i^2 = v_{2i}$ for $2i < M$ and $v_i^2 = 0$ for $2i \geq M$ and $\text{Sq}^1 v_{2i} = v_{2i+1}$ for $2i+1 < M$. All torsion in $H^*(\text{SO}(M)/\text{SO}(m))$ is 2-torsion and the torsion ideal has a canonical free abelian complement admitting a simple system of generators. This simple system consists of the following nontorsion generators indexed by degree:*

$$q_{4j-1} \text{ whenever } [2j-1, 2j+1] \subseteq [m, M], \quad u_m \text{ if } m \text{ is even,} \quad \chi_{2\ell-1} \text{ if } M = 2\ell.$$

The squares of these generators are 2-torsion, and particularly the squares u_m^2 and $\chi_{2\ell-1}^2$ are 0.

One has $\rho\chi_{2\ell-1} = v_{2\ell-1}$. Given $N < M$, the maps induced by the inclusion $\text{SO}(N)/\text{SO}(m) \rightarrow \text{SO}(M)/\text{SO}(m)$ are surjective on the v_i , the q_{4j-1} , and u_m , but $\chi_{2\ell-1}$ is not in the image. When $M = 2\ell$ is even and $M > n > m$, the map induced in cohomology by the quotient map $\text{SO}(M)/\text{SO}(m) \rightarrow \text{SO}(M)/\text{SO}(n)$ does preserve $\chi_{2\ell-1}$. The transgression of $\chi_{2\ell-1}$ in the Serre spectral sequence of the universal principal $\text{SO}(2\ell)$ -bundle is a non-torsion class $e_{2\ell} \in H^{2\ell} \text{BSO}(2\ell)$, the *Euler class*, which is annihilated by restriction along the maps $\text{BSO}(N) \rightarrow \text{BSO}(2\ell)$ for $N < 2\ell$.

We will show that, similarly, both $\overline{H}^*(F_{\text{SO}})$ and $H^*(F_{\text{SO}}; \mathbb{F}_2)$ admit simple systems of generators and $H^*(F_{\text{SO}})$ has only 2-torsion. To state the result precisely it will help to expand our graphical lexicon.

Notation 5.3.10. We refer to as a \triangleleft -shape any three consecutive rows $k, k+1, k+2$ in an orthogonal Gelfand–Zeitlin pattern such that the full subgraph on the white components in these rows is made up of a \triangleleft -shape in rows k and $k+1$ and an \triangleleft -shape in rows $k+1$ and $k+2$. For either of the shapes \triangleleft and \triangleleft , we will use subscript labels to refer to the width ℓ , counted in vertices, of the bottom row of the shape, or the parity $\bar{\ell} = \ell \bmod 2$ of this width.

We refer to as a (white) \square -shape the full subgraph of a white component of an orthogonal Gelfand–Zeitlin pattern bounded by (and including) two rows whose widths are consecutive local maxima. If the top row is of locally maximum width, it *does not count* as a hexagon. To a \square -shape of width M vertices at its longest row and m vertices at its top row, we assign the *associated Stiefel manifold* $\text{SO}(M)/\text{SO}(m) = V_{M-m}(\mathbb{R}^M)$, visible as a fiber in (5.3.4).

²² Even integral cohomology ring of $\text{SO}(k)$ is involved, and has been known in full only since the late 1980s [Pit91].

²³ For example, the polynomial ring $\mathbb{Z}[x]$ admits the simple system of generators x^{2^j} . If A itself admits a simple system of generators, then its ring structure is determined entirely by the existence of the simple system of generators and the values of the squares v_j^2 .

Examples 5.3.11. There are two \mathbf{A} -shapes in Figure 3.5.17a, in the upper half of the white diamond, and precisely one \mathbf{A} -shape in each member of the family in Figures 3.5.17b to 3.5.17d yielding GZ fibers $V_2(\mathbb{R}^m)$. The pattern in Figure 3.5.17a has a $\mathbf{\Delta}_0$ -shape, more specifically a $\mathbf{\Delta}_4$ -shape, in rows 4 and 5, and a \mathbf{A}_3 -shape above in rows 5, 6, 7. In each of the patterns in Figure 3.5.17 and in Figure 2.3.8 there is precisely one \mathbf{O} -shape, and in Figure 5.3.15 there are five.

Theorem 5.3.12. *All torsion in the cohomology of F_{SO} (Notation 5.3.1) is 2-torsion. If V_p are the Stiefel manifolds associated to the white \mathbf{O} -shapes of the Gelfand–Zeitlin-pattern in Notation 5.3.10 and (5.3.4), one has graded group isomorphisms*

$$H^*(F_{\text{SO}}) \cong H^*\left(\prod_{p=1}^r V_p\right) \quad \text{and} \quad H^*(F_{\text{SO}}; \mathbb{F}_2) \cong \bigotimes_{p=1}^r H^*(V_p; \mathbb{F}_2)$$

and a graded ring isomorphism

$$\overline{H}^*(F_{\text{SO}}) \cong \bigotimes \overline{H}^*(V_p) \cong \Lambda[z_{s_i}, q_{4s'_j-1}], \quad |z_{s_i}| = s_i, \quad |q_{4s'_j-1}| = 4s'_j - 1,$$

where the generators $q_{4s'_j-1}$ are indexed by the white $\mathbf{A}_{2s'_j+1}$ -shapes in the Gelfand–Zeitlin pattern and the generators z_{s_i} are indexed by the set of those white $\mathbf{\Delta}_{s_i+1}$ -shapes not contained in any \mathbf{A}_1 -shape.²⁴

Some, but not all, of the multiplicative structure of the $H^*(V_p)$ is visible in $H^*(F_{\text{SO}})$. If we are willing to discard multiplicative information altogether, we have an additive characterization that is even simpler.

Corollary 5.3.13. *As a graded group, $H^*(F_{\text{SO}})$ is isomorphic to the cohomology of a direct product of Stiefel manifolds $V_2(\mathbb{R}^{2s'_j+1})$ indexed by $\mathbf{A}_{2s'_j+1}$ -shapes and of spheres S^{s_i} indexed by $\mathbf{\Delta}_{s_i+1}$ -shapes not contained in any \mathbf{A}_1 -shape.*

Before diving into the proof, we give one last example.

Example 5.3.14. Consider an orthogonal GZ pattern with white component outlined in Figure 5.3.15, where rows of locally maximal or minimal width are labeled by their widths. One has an expression $F_{\text{SO}}^{22} \cong X \otimes_{\text{SO}(1)} Y = X \times Y$, where X and Y are the spaces corresponding to the subpatterns joined at the pinch point of width 1.

Counting \mathbf{A}_1 -shapes, we find a \mathbf{A}_3 -shape (a triangle) contributing a $V_2(\mathbb{R}^3) = \text{SO}(3)$ factor in cohomology and a disjoint $\mathbf{\Delta}_3$ -shape contributing an S^2 factor. Counting all $\mathbf{\Delta}$ -shapes, we find two $\mathbf{\Delta}_3$'s and an $\mathbf{\Delta}_2$, so $H^*(X; \mathbb{F}_2)$ admits a simple system of generators of orders 2, 2, 1. For the ring structure, the balanced product description

$$X \cong \text{SO}(1) \underset{\text{SO}(1)}{\otimes} \text{SO}(3) \underset{\text{SO}(2)}{\otimes} \text{SO}(3)/\text{SO}(1) \cong \text{SO}(3) \underset{\text{SO}(2)}{\otimes} \text{SO}(3).$$

gives the sequence of Stiefel manifolds $\text{SO}(3)/\text{SO}(2) \cong S^2$ and $\text{SO}(3)/\text{SO}(1) \cong \text{SO}(3)$ corresponding to the \mathbf{O} -shapes. In this case the diffeomorphism $g \otimes h \mapsto (g\text{SO}(2), gh)$ gives us $S^2 \times \text{SO}(3)$.

Similarly, reading up from the bottom of the other component Y for \mathbf{O} -shapes, we find the Stiefel manifolds $S^7 \cong \text{SO}(8)/\text{SO}(7)$, $V_2 = \text{SO}(8)/\text{SO}(6)$, and $V_3 = \text{SO}(7)/\text{SO}(3)$. In the balanced product description

$$Y \cong \text{SO}(1) \underset{\text{SO}(1)}{\otimes} \text{SO}(8) \underset{\text{SO}(7)}{\otimes} \text{SO}(8) \underset{\text{SO}(6)}{\otimes} \text{SO}(7)/\text{SO}(3),$$

²⁴ For ease of presentation, we allow even-dimensional exterior generators, meaning central elements squaring to 0.

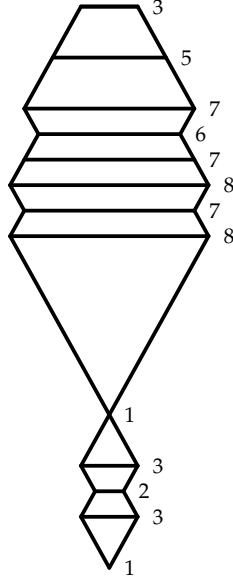


Figure 5.3.15: Outline of a white component of a GZ pattern on a non-regular coadjoint orbit of $\mathrm{SO}(22)$; the numerical labels are row width in number of vertices.

the first Stiefel manifold S^7 splits off to leave $\mathrm{SO}(8) \otimes_{\mathrm{SO}(6)} \mathrm{SO}(7)/\mathrm{SO}(3)$, a V_3 -bundle over V_2 . Reading the remaining two \square -shapes, corresponding to V_2 and V_3 , for \mathbf{A}_1 -shapes, we find a \mathbf{A}_7 and a \mathbf{A}_5 , respectively giving factors $H^*V_2(\mathbb{R}^7)$ and $H^*V_2(\mathbb{R}^5)$. Then looking for Δ -shapes not contained in these, one encounters, reading from the bottom, two Δ_8 's and a Δ_7 , respectively contributing two S^7 factors and an S^6 . Thus Y has the cohomology of $S^7 \times S^7 \times S^6 \times V_2(\mathbb{R}^7) \times V_2(\mathbb{R}^5)$ additively over \mathbb{Z} and \mathbb{F}_2 , and multiplicatively over \mathbb{Z} after quotienting out 2-torsion.

Proof of Lemma 5.3.5. A result of Borel [Bor53, Prop. 8.2] states that given a bundle $F \rightarrow E \rightarrow B$ of compact CW complexes such that all torsion in $H^*(F)$ and $H^*(B)$ is 2-torsion and the rational and mod-2 Serre spectral sequences collapse, the integral spectral sequence also collapses without an extension problem, so that as graded groups, one has $H^*(E) \cong E_\infty = E_2 \cong H^*(B \times F)$. We will show that each Serre spectral sequence collapses over \mathbb{Q} and \mathbb{F}_2 , and then it will follow by induction starting with Proposition 5.3.9 and the Künneth theorem that all torsion in each $H^*(F^{\ell_p})$ is 2-torsion and each Serre spectral sequence collapses integrally.

Fix $p \in [1, r]$. Letting N be the largest of the M_t for $t \in [1, p]$, we observe that $\prod_t \mathrm{SO}(M_t)$ is a subgroup of $\mathrm{SO}(M)^p$, where $M_{\ell_r} = 2\ell$, and that the iterated group multiplication $(g_1, \dots, g_p) \mapsto g_1 \cdots g_p$ on $\mathrm{SO}(N)$ restricts to a map $\prod_t \mathrm{SO}(M_t) \rightarrow \mathrm{SO}(N)$. By the definition of the balanced product, this multiplication descends to a well-defined map

$$\begin{aligned} \mu_p: F^{\ell_p} = \mathrm{SO}(M_1) \otimes_{\mathrm{SO}(m_1)} \mathrm{SO}(M_2) \otimes_{\mathrm{SO}(m_2)} \cdots \otimes_{\mathrm{SO}(m_{p-1})} \mathrm{SO}(M_p)/\mathrm{SO}(m_p) &\longrightarrow \mathrm{SO}(N)/\mathrm{SO}(m_p), \\ g_1 \otimes \cdots \otimes g_p \mathrm{SO}(m_p) &\longmapsto g_1 \cdots g_p \mathrm{SO}(m_p). \end{aligned}$$

It is clear that following the fiber inclusion

$$\begin{aligned} i_p: \mathrm{SO}(M_p)/\mathrm{SO}(m_p) = V_p &\longrightarrow F^{\ell_p}, \\ g_p \mathrm{SO}(m_p) &\longmapsto 1 \otimes \cdots \otimes 1 \otimes g_p \mathrm{SO}(m_p). \end{aligned}$$

with μ_p gives the standard injection $\mathrm{SO}(M_p)/\mathrm{SO}(m_p) \rightarrow \mathrm{SO}(N)/\mathrm{SO}(m_p)$ discussed in Proposition 5.3.9. Thus each generator v_i lies in the image of i_p^* , hence i_p^* is surjective onto $H^*(V_p; \mathbb{F}_2)$ and the mod-2 Serre spectral sequence collapses. This already gives the mod-2 isomorphism.

To prove the rational collapse, note each q_{4j-1} is also in the image of i_p^* , as is u_{m_p} when m_p is even. It remains only to find a lift in $H^{2s-1}(F^{\ell_p}; \mathbb{Q})$ of $\chi_{2s-1} \in H^{2s-1}(\mathrm{SO}(M_p)/\mathrm{SO}(m_p); \mathbb{Q})$ if $M_p = 2s$ is even. Abbreviate the balanced product of the first $p-1$ factors in (3.5.9) as X , so that F^{ℓ_p} is $X \otimes_{\mathrm{SO}(m_{p-1})} \mathrm{SO}(2s)/\mathrm{SO}(m_p)$. Since the actions of $\mathrm{SO}(m_{p-1})$ and $\mathrm{SO}(m_p)$ are free, F^{ℓ_p} is homotopy equivalent to the homotopy orbit space

$$F' := X \otimes_{\mathrm{SO}(m_{p-1})} (\mathrm{ESO}(2s) \times \mathrm{SO}(2s) \otimes_{\mathrm{SO}(m_p)} \mathrm{ESO}(2s)),$$

where the action of $\mathrm{SO}(m_{p-1})$ on the right-hand factor is by $g \cdot (e, h \otimes e') := (eg^{-1}, gh \otimes e')$. We can then replace V_p by $V' := \mathrm{SO}(2s) \otimes_{\mathrm{SO}(m_p)} \mathrm{ESO}(2s)$, replace i_p by the obvious map $i': h \otimes e' \mapsto x_0 \otimes (e_0, h \otimes e')$ for fixed basepoints $x_0 \in X$ and $e_0 \in \mathrm{ESO}(2s)$, and replace the quotient map $\mathrm{SO}(2s) \rightarrow V_p$ by $\pi': h \mapsto h \otimes e_0$.

There are natural quotient maps from F' to

$$F'' := X \otimes_{\mathrm{SO}(m_{p-1})} (\mathrm{ESO}(2s) \times \mathrm{SO}(2s) \otimes_{\mathrm{SO}(2s-1)} \mathrm{ESO}(2s))$$

and from V' to $V'' := \mathrm{SO}(2s) \otimes_{\mathrm{SO}(2s-1)} \mathrm{ESO}(2s) \simeq S^{2s-1}$. Dropping the X coordinate in F'' yields a natural quotient map ω to $E := \mathrm{ESO}(2s) \otimes_{\mathrm{SO}(m_{p-1})} \mathrm{SO}(2s) \otimes_{\mathrm{SO}(2s-1)} \mathrm{ESO}(2s)$. These maps then fit together as follows:

$$\begin{array}{ccccc} \mathrm{SO}(2s) & \xrightarrow{\pi'} & V' & \xrightarrow{\pi} & V'' \\ & & \downarrow i' & & \downarrow i \\ & & F' & \xrightarrow{\omega'} & F'' \xrightarrow{\omega} E. \end{array}$$

To lift $\chi_{2s-1} \in H^{2s-1}(V_p; \mathbb{Q}) \cong H^{2s-1}(V'; \mathbb{Q})$ to $F^{\ell_p} \simeq F'$, it is enough by commutativity of the square to find a lift to F'' along $i \circ \pi$. Now by Proposition 5.3.9, the fundamental class of $V'' \simeq S^{2s-1}$ is the unique lift of χ_{2s-1} under π^* and also the unique lift of $\tilde{\chi} = (\pi')^* \chi_{2s-1} \in H^{2s-1}(\mathrm{SO}(2s); \mathbb{Q})$ under $(\pi \circ \pi')^*$, so it will be enough to see $\tilde{\chi}$ lies in the image of the fiber restriction along $\omega \circ i \circ \pi \circ \pi'$.

For this, we note that this map is a fiber inclusion of the nonprincipal $\mathrm{SO}(2s)$ -bundle $E \rightarrow \mathrm{BSO}(m_{p-1}) \times \mathrm{BSO}(2s-1)$ with projection $e \otimes g \otimes e' \mapsto (e\mathrm{SO}(m_{p-1}), \mathrm{SO}(2s-1)e')$. We will show that $\tilde{\chi}$ transgresses to 0 in the Serre spectral sequence of this bundle, so that it lies in the image of the fiber restriction. Following Eschenburg [Esch92], consider the following square:

$$\begin{array}{ccc} E = \mathrm{ESO}(2s) \otimes_{\mathrm{SO}(m_{p-1})} \mathrm{SO}(2s) \otimes_{\mathrm{SO}(2s-1)} \mathrm{ESO}(2s) & \xrightarrow{\tilde{\kappa}} & \mathrm{ESO}(2s) \otimes_{\mathrm{SO}(2s)} \mathrm{SO}(2s) \otimes_{\mathrm{SO}(2s)} \mathrm{ESO}(2s) \simeq \mathrm{BSO}(2s) \\ \downarrow & & \downarrow \\ \mathrm{BSO}(m_{p-1}) \times \mathrm{BSO}(2s-1) & \xrightarrow{\kappa} & \mathrm{BSO}(2s) \times \mathrm{BSO}(2s). \end{array}$$

The right vertical map $e \otimes g \otimes e' \mapsto (\mathrm{SO}(2s)e, e'\mathrm{SO}(2s))$ is the projection of another $\mathrm{SO}(2s)$ -bundle and by inspection the horizontal map $e \otimes g \otimes e' \mapsto e \otimes g \otimes e'$ makes the square a map of $\mathrm{SO}(2s)$ -bundles such that the map κ of base spaces is up to homotopy that induced functorially by the subgroup inclusions. The projection of the right bundle is, up to homotopy, the

diagonal map on $BSO(2s)$, which induces the cup product in cohomology, and so in the Serre spectral sequence of the right bundle, $\tilde{\chi} \in E_2^{0,2s-1} \cong H^{2s-1}(\mathrm{SO}(2s); \mathbb{Q})$ transgresses to the image in $E_2^{2s,0}$ of the element $1 \otimes e_{2s} - e_{2s} \otimes 1$ of $E_2^{2s,0} \cong \bigoplus_{a+b=2s} H^a(BSO(2s); \mathbb{Q}) \otimes_{\mathbb{Q}} H^b(BSO(2s); \mathbb{Q})$. The map of fiber bundles induces a map $(E_r(\tilde{\kappa}))_r$ of spectral sequences, so in the left spectral sequence, $\tilde{\chi}$ transgresses to the $E_2^{2s,0}(\tilde{\kappa})$ -image of this element. But e_{2s} lies in the kernel of $H^*(BSO(2s); \mathbb{Q}) \rightarrow H^*(BSO(t); \mathbb{Q})$ for $t < 2s$ by Proposition 5.3.9, and $2s-1, m_{p-1} < M_p = 2s$, so $E_2^{2s,0}(\tilde{\kappa}) = H^{2s}(\kappa; H^0(\mathrm{id}_{\mathrm{SO}(2s)}; \mathbb{Q}))$ annihilates this image and hence $\tilde{\chi}$ transgresses to 0 as claimed. It is thus the image of some x in $H^{2s-1}(E; \mathbb{Q})$ and our desired lift in $H^{2s-1}(F^{\ell_p}; \mathbb{Q})$ is $(\omega \circ \omega')^* x$. \square

Proof of Theorem 5.3.12. The integral statement follows from Borel's theorem cited in the proof of Lemma 5.3.5. For the statement about $\overline{H}^*(F_{\mathrm{SO}})$, we show inductively that each $\overline{H}^*(V_p)$ is exterior. Particularly, $\overline{H}^*(V_1)$ is by Proposition 5.3.9, so inductively assume the same of $\overline{H}^*(F^{\ell_{p-1}})$. The Serre spectral sequence of $V_p \rightarrow F^{\ell_p} \rightarrow F^{\ell_{p-1}}$ modulo torsion collapses at $E_2 = \overline{H}^*(F^{\ell_{p-1}}) \otimes \overline{H}^*(V_p)$, so we need only to lift a system of exterior generators from $\overline{H}^*(V_p)$. For these we take the various images $\mu_p^* q_{4j-1}$, and additionally $(\omega \circ \omega')^* x$ if M_p is even²⁵ and $\mu_p^* u_{m_p}$ if u_{m_p} is even, which works because $u_{m_p}^2 = 0$ in $H^{2m_p}(\mathrm{SO}(N)/\mathrm{SO}(m_p))$.

It remains to enumerate these generators by trapezoids. This follows on examining each $V_p = \mathrm{SO}(M_p)/\mathrm{SO}(m_p)$ separately. Write M' for M_p itself if it is odd and otherwise for $M_p - 1$, and similarly m' for m_p itself if it is odd and otherwise for $m_p + 1$. Then there is a bundle tower

$$\begin{array}{ccccccc} \frac{\mathrm{SO}(m')}{\mathrm{SO}(m_p)} & \frac{\mathrm{SO}(m'+2)}{\mathrm{SO}(m')} & \frac{\mathrm{SO}(m'+4)}{\mathrm{SO}(m'+2)} & \cdots & \frac{\mathrm{SO}(M'-2)}{\mathrm{SO}(M'-4)} & \frac{\mathrm{SO}(M')}{\mathrm{SO}(M'-2)} & \\ \downarrow & \downarrow & \downarrow & & \downarrow & \downarrow & \\ V_p & \rightarrow \frac{\mathrm{SO}(M_p)}{\mathrm{SO}(m')} & \rightarrow \frac{\mathrm{SO}(M_p)}{\mathrm{SO}(m'+2)} & \rightarrow \cdots & \rightarrow \frac{\mathrm{SO}(M_p)}{\mathrm{SO}(M'-4)} & \rightarrow \frac{\mathrm{SO}(M_p)}{\mathrm{SO}(M'-2)} & \rightarrow \frac{\mathrm{SO}(M_p)}{\mathrm{SO}(M')} \end{array}$$

Borel showed [Bor53, Prop. 10.4] that the cohomology of V_p and of the direct product of the fibers and the base in this diagram are isomorphic. Quotienting out torsion, the cohomology of each fiber and the base space become exterior, on generators, displayed respectively from left to right,

$$(u_{m_p}) \quad q_{2m'+1}, \quad q_{2m'+5}, \quad \cdots, \quad q_{2M'-7}, \quad q_{2M'-3}, \quad (\chi_{M_{p-1}})$$

where u_{m_p} is contributed if and only if the last fiber is nontrivial, which is to say, m_p is even, and $\chi_{M_{p-1}}$ is contributed if and only if the base is nontrivial, which is to say, M_p is even. Now the fibers $\mathrm{SO}(M' - 2t)/\mathrm{SO}(M' - 2t - 2)$ correspond to $\mathbf{\Delta}$ -shapes of (odd) width $M' - 2t$ and $\mathrm{SO}(m')/\mathrm{SO}(m_p)$ and $\mathrm{SO}(M_p)/\mathrm{SO}(M')$ correspond to the possible leftover $\mathbf{\Delta}$ -shapes of respective widths m' and M_p on the top and bottom of the white \square -shape associated to V_p . \square

We do not hope to give a simple presentation for $H^*(F_{\mathrm{SO}})$ or even $H^*(F_{\mathrm{SO}}; \mathbb{F}_2)$, but the mod-2 homology admits a nice description following the same reasoning as Proposition 5.2.5.

Proposition 5.3.16. *The quotient map*

$$\pi : \prod_{p=1}^r \mathrm{SO}(M_p) \longrightarrow \mathrm{SO}(M_1) \otimes_{\mathrm{SO}(m_1)} \cdots \otimes_{\mathrm{SO}(m_{r-1})} \mathrm{SO}(M_r)/\mathrm{SO}(m_r) = F_{\mathrm{SO}}$$

²⁵ Since there is no longer any 2-torsion, for the odd-degree lifts we could really have taken anything.

induces a surjection in mod-2 homology and an identification

$$H_*(F_{\text{SO}}; \mathbb{F}_2) \cong H_*(\text{SO}(M_1); \mathbb{F}_2) \otimes_{H_*(\text{SO}(m_1); \mathbb{F}_2)} \cdots \otimes_{H_*(\text{SO}(m_{r-1}); \mathbb{F}_2)} H_*(\text{SO}(M_r); \mathbb{F}_2) \otimes_{H_*(\text{SO}(m_r); \mathbb{F}_2)} \mathbb{F}_2.$$

Dually, π induces an injection in mod-2 cohomology.

Remark 5.3.17. One even has π^* an injection integrally if none of the m_p except possibly m_r are even, because the lifts of q_{4j-1} and χ_{2s-1} for $M_p = 2s$ inject under π^* ; but $\pi^*u_{m_p}$ is 2-torsion for m_p even.

Example 5.3.18. Recall that we promised in Remark 3.5.11 a counterexample to the most optimistic possible claim about the structure the cohomology ring of $X = \text{SO}(9) \otimes_{\text{SO}(5)} \text{SO}(6)/\text{SO}(2)$. Pulling back along the quotient map μ_1 to $V_1 = \text{SO}(9)/\text{SO}(5)$ we get four generators v'_8, v'_7, v'_6, v'_5 . There is no map to $V_2 = \text{SO}(6)/\text{SO}(2)$, but pulling back along the multiplication map μ_2 to $\text{SO}(9)/\text{SO}(3)$ we get three more generators v''_5, v''_4, v''_3 . These seven classes form a simple system of generators for $H^*(X; \mathbb{F}_2)$ whose respective images in $H^*(\text{SO}(9) \times \text{SO}(6); \mathbb{F}_2)$ under the embedding π^* of Proposition 5.3.16 are

$$v_8 \otimes 1, \quad v_7 \otimes 1, \quad v_6 \otimes 1, \quad v_5 \otimes 1, \quad v_5 \otimes 1 + 1 \otimes v_5, \quad v_4 \otimes 1 + 1 \otimes v_4, \quad v_3 \otimes 1 + 1 \otimes v_3.$$

In particular, we see $(v''_4)^2 = v'_8$. Since v''_4 lies in the image of μ_2^* but not in that of μ_1^* and v'_8 lies in the image of μ_1^* but not of μ_2^* , there is no way to arrange a ring isomorphism $H^*(F_{\text{SO}}; \mathbb{F}_2) \cong H^*(V_1 \times V_2; \mathbb{F}_2)$.

Integrally, we have a simple system of generators $q'_{15}, q'_{11}, \chi''_5, q''_7$ for the free abelian summand, and in particular $\overline{H}^8(F_{\text{SO}}) = 0$. Now $v''_4 = \text{Sq}^1 v''_3 = \rho \beta v''_3$ and $v'_8 = \text{Sq}^1 v'_7 = \rho \beta v'_7$ are reductions of integral classes, and ρ is a ring homomorphism injective on torsion, so it follows that $(\beta v''_3)^2 = \beta v'_7$ in $H^8(F_{\text{SO}})$. Thus we cannot have a ring isomorphism $H^*(F_{\text{SO}}) \cong H^*(V_1 \times V_2)$.

Remark 5.3.19. The description of a GZ fiber as a product of biquotients (hence a biquotient itself) from Proposition 3.4.13 makes available a different closed-form expression for the cohomology of such spaces. Singhof [Sing93] observed that a biquotient $K \backslash G / H$ of compact, connected Lie groups can be expressed up to homotopy as the homotopy pullback of the diagram $BK \rightarrow BG \leftarrow BH$, to which Munkholm's general Eilenberg–Moore collapse result [Munk74] applies to yield

$$H^*(K \backslash G / H; k) \cong \text{Tor}_{H^*(BG; k)}^*(H^*(BK; k), H^*(BH; k)) \quad (5.3.20)$$

as graded modules over any principal ideal domain k of characteristic $\neq 2$ such that the cohomology rings of BG, BK, BH are polynomial. Vitali Kapovitch [Kap04], building on work of Eschenburg [Esch92], showed (5.3.20) holds as a ring isomorphism for $k = \mathbb{Q}$, and the first author recently found, using A_∞ -algebraic techniques and a product due to Franz on a two-sided bar construction, that the isomorphism (5.3.20) is multiplicative so long as 2 is a unit of k [CF21].

Since $H^*U(n)$ is free abelian and $H^*\text{SO}(n)$ has torsion only of order two, (5.3.20) determines the cohomology ring of any unitary GZ fiber (or orthogonal GZ fiber for $k = \mathbb{Z}[1/2]$). For a general biquotient, knowing (5.3.20) greatly simplifies life since the Tor in question is algorithmically computable using a finitely generated Koszul complex, but in the present case, it is easier still to simply read the ring structure off the GZ pattern.

References

- [Ala09] I. Alamiidine. *Géométrie de systèmes hamiltoniens intégrables: Le cas du système de Gelfand-Ceitlin*. PhD thesis, Université Toulouse, 2009. <http://thesesups.ups-tlse.fr/538>.
- [BMMT18] A. Bolsinov, V. S. Matveev, E. Miranda, and S. Tabachnikov. Open problems, questions and challenges in finite-dimensional integrable systems. *Philos. Trans. Roy. Soc. A*, 376, 2018. [arXiv:1804.03737](https://arxiv.org/abs/1804.03737), [doi:10.1098/rsta.2017.0430](https://doi.org/10.1098/rsta.2017.0430).
- [Bor53] A. Borel. Sur la cohomologie des espaces fibrés principaux et des espaces homogènes de groupes de Lie compacts. *Ann. of Math.* (2), 57(1):115–207, 1953. <http://web.math.rochester.edu/people/faculty/doug/otherpapers/Borel-Sur.pdf>, [doi:10.2307/1969728](https://doi.org/10.2307/1969728).
- [Bor54] Armand Borel. Sur l’homologie et la cohomologie des groupes de Lie compacts connexes. *American J. Math.*, pages 273–342, 1954. [doi:10.2307/2372574](https://doi.org/10.2307/2372574).
- [Bou18] D. Bouloc. Singular fibers of the bending flows on the moduli space of 3D polygons. *J. Symplectic Geom.*, 16(3):585 – 629, 2018. [arXiv:1505.04748](https://arxiv.org/abs/1505.04748), [doi:10.4310/JSG.2018.v16.n3.a1](https://doi.org/10.4310/JSG.2018.v16.n3.a1).
- [BouMZ18] D. Bouloc, E. Miranda, and N. T. Zung. Singular fibers of the Gelfand-Ceitlin system on $u(n)^*$. *Philos. Trans. Roy. Soc. A*, 376, 2018. [arXiv:1803.08332](https://arxiv.org/abs/1803.08332), [doi:10.1098/rsta.2017.0423](https://doi.org/10.1098/rsta.2017.0423).
- [ČaMV03] M. Čadek, M. Mimura, and J. Vanžura. The cohomology rings of real Stiefel manifolds with integer coefficients. *J. Math. Kyoto Univ.*, 43(2):411–428, 2003. [doi:10.1215/kjm/1250283733](https://doi.org/10.1215/kjm/1250283733).
- [CF21] J. D. Carlson (appendix joint with M. Franz). The cohomology of biquotients via a product on the two-sided bar construction (expository version). 2021. [arXiv:2106.02986](https://arxiv.org/abs/2106.02986).
- [CK20] Y. Cho and Y. Kim. Lagrangian fibers of Gelfand–Cetlin systems of $SO(n)$ -type. *Transform. Groups*, May 2020. [arXiv:1806.01529](https://arxiv.org/abs/1806.01529), [doi:10.1007/s00031-020-09566-4](https://doi.org/10.1007/s00031-020-09566-4).
- [CKO20] Y. Cho, Y. Kim, and Y.-G. Oh. Lagrangian fibers of Gelfand–Cetlin systems. *Adv. Math.*, 372, 2020. [arXiv:1911.04132](https://arxiv.org/abs/1911.04132), [doi:10.1016/j.aim.2020.107304](https://doi.org/10.1016/j.aim.2020.107304).
- [Esch92] J.-H. Eschenburg. Cohomology of biquotients. *Manuscripta Math.*, 75(2):151–166, 1992. [doi:10.1007/BF02567078](https://doi.org/10.1007/BF02567078).
- [Gold86] W. M. Goldman. Invariant functions on Lie groups and Hamiltonian flows of surface group representations. *Invent. Math.*, 85(2):263–302, June 1986. [doi:10.1007/BF01389091](https://doi.org/10.1007/BF01389091).
- [GS83a] V. Guillemin and S. Sternberg. The Gelfand–Cetlin system and quantization of the complex flag manifolds. *J. Funct. Anal.*, 52(1):106–128, 1983. [doi:10.1016/0022-1236\(83\)90092-7](https://doi.org/10.1016/0022-1236(83)90092-7).
- [GS83b] V. Guillemin and S. Sternberg. On collective complete integrability according to the method of Thimm. *Ergodic Theory Dynam. Systems*, 3(2):219–230, 1983. [doi:10.1017/S0143385700001930](https://doi.org/10.1017/S0143385700001930).
- [HK14] M. D. Hamilton and H. Konno. Convergence of Kähler to real polarizations on flag manifolds via toric degenerations. *J. Symplectic Geom.*, 12(3):473–509, September 2014. [arXiv:1105.0741](https://arxiv.org/abs/1105.0741), [doi:10.4310/JSG.2014.v12.n3.a3](https://doi.org/10.4310/JSG.2014.v12.n3.a3).
- [HK15] M. Harada and K. Kaveh. Integrable systems, toric degenerations and Okounkov bodies. *Invent. Math.*, 202(3):927–985, 2015. [doi:10.1007/s00222-014-0574-4](https://doi.org/10.1007/s00222-014-0574-4).
- [HL20] B. Hoffman and J. Lane. Stratified gradient Hamiltonian vector fields and collective integrable systems. October 2020. [arXiv:2008.13656](https://arxiv.org/abs/2008.13656).
- [KaKLS20] S. Kaji, S. Kuroki, E. Lee, and D. Y. Suh. Flag Bott manifolds of general Lie type and their equivariant cohomology rings. *Homology Homotopy Appl.*, 22(1):375–390, 2020. [arXiv:1905.00303](https://arxiv.org/abs/1905.00303), [doi:10.4310/HHA.2020.v22.n1.a21](https://doi.org/10.4310/HHA.2020.v22.n1.a21).
- [Kap04] V. Kapovitch. A note on rational homotopy of biquotients. 2004. <http://math.toronto.edu/vtk/biquotient.pdf>.
- [KapM96] M. Kapovich and J. Millson. The symplectic geometry of polygons in Euclidean space. *J. Differential Geom.*, 44(3):479–513, 1996.
- [Lane18] J. Lane. Convexity and Thimm’s trick. *Transform. Groups*, 23:963 – 987, 2018. [arXiv:1509.07356](https://arxiv.org/abs/1509.07356), [doi:10.1007/s00031-017-9436-7](https://doi.org/10.1007/s00031-017-9436-7).

- [Munk74] Hans J. Munkholm. The Eilenberg–Moore spectral sequence and strongly homotopy multiplicative maps. *J. Pure Appl. Algebra*, 5(1):1–50, 1974. doi:10.1016/0022-4049(74)90002-4.
- [NNU10] T. Nishinou, Y. Nohara, and K. Ueda. Toric degenerations of Gelfand–Cetlin systems and potential functions. *Adv. Math.*, 224(2), 2010. arXiv:0810.3470, doi:10.1016/j.aim.2009.12.012.
- [NU16] Y. Nohara and K. Ueda. Floer cohomologies of non-torus fibers of the Gelfand–Cetlin system. *J. Symplectic Geom.*, 14(4):1251–1293, 2016. arXiv:1409.4049, doi:10.4310/JSG.2016.v14.n4.a9.
- [Pab12] M. Pabiniak. *Hamiltonian Torus Actions in Equivariant Cohomology and Symplectic Topology*. PhD thesis, Cornell University, 2012. <http://pi.math.cornell.edu/~milena/thesis.pdf>.
- [Pit91] H. V. Pittie. The integral homology and cohomology rings of $SO(n)$ and $Spin(n)$. *J. Pure Appl. Algebra*, 73(2):105–153, 1991. doi:10.1016/0022-4049(91)90108-E.
- [Sing93] W. Singhof. On the topology of double coset manifolds. *Math. Ann.*, 297(1):133–146, 1993. doi:10.1007/BF01459492.

DEPARTMENT OF MATHEMATICS,
IMPERIAL COLLEGE LONDON
j.carlson@imperial.ac.uk

DEPARTMENT OF MATHEMATICS & STATISTICS,
McMASTER UNIVERSITY
lanej5@math.mcmaster.ca